



Modelling inter-aquifer leakage associated with well integrity failure

Rebecca Doble, Jim McCallum, Chris Turnadge, Luk Peeters, Bailin Wu, Dirk Mallants

This report was commissioned by the Department of the Environment and Energy and was prepared by CSIRO.

2018

Copyright

© Commonwealth Scientific and Industrial Research Organisation 2018. To the extent permitted by law, all rights are reserved and no part of this publication covered by copyright may be reproduced or copied in any form or by any means except with the written permission of CSIRO.

Citation

This report should be cited as:

Doble R, McCallum J, Turnadge C, Peeters, L., Wu B, Mallants D (2018). Modelling inter-aquifer leakage associated with well integrity failure, prepared by the Commonwealth Scientific and Industrial Research Organisation (CSIRO), Canberra.

Acknowledgements

This report was subject to review processes during its development. We specifically acknowledge Professor Jim Unterschultz (University of Queensland), Professor Craig Simmons (Flinders University of South Australia) and Scott Lawson (Department of the Environment and Energy) for their contributions to the review.

Important disclaimer

CSIRO advises that the information contained in this publication comprises general statements based on scientific research. The reader is advised and needs to be aware that such information may be incomplete or unable to be used in any specific situation. No reliance or actions must therefore be made on that information without seeking prior expert professional, scientific and technical advice. To the extent permitted by law, CSIRO (including its employees and consultants) excludes all liability to any person for any consequences, including but not limited to all losses, damages, costs, expenses and any other compensation, arising directly or indirectly from using this publication (in part or in whole) and any information or material contained in it.

CSIRO is committed to providing web accessible content wherever possible. If you are having difficulties with accessing this document please contact enquiries@csiro.au.

Table of Contents

Table of Contents	iii
-------------------------	-----

List of Figures	v
List of Tables	vii
Executive summary	viii
Abbreviations	x
Glossary	xi
Symbols	xiii
1 Introduction	1
2 Conceptualisation of leaky wells	3
2.1 Seepage pathway conceptualisation	3
2.2 Exploring the potential impact space with analytical solutions	5
2.3 Well hydraulic properties.....	5
2.4 Well hydraulic gradient.....	6
3 Numerical model development	16
4 Results	20
4.1 Comparison numerical - analytical solutions.....	20
4.2 Impact of cell dimensions	20
4.3 Metric 1: Comparison between flow through the well and flow through the aquitard	21
4.4 Metric 2: Impacts of the leaky well on aquifer recovery.....	22
4.4.1 Scenario 1: baseline without leaky wells.....	22
4.4.2 Scenario 2: Leaky well.....	24
4.4.3 Scenario 3: Open well	25
4.5 Metric 3: head changes around a well.....	26
4.5.1 Scenario 1: baseline without leaky wells.....	26
4.5.2 Scenario 2: Leaky well.....	28

4.5.3 Scenario 3: Open well 30

5	Discussion	33
6	Conclusions	35
7	References	36

List of Figures

Figure 1 Pathways for water movement in cemented wellbores: flow through microannulus between cement and rock matrix (1) or steel casing (2), flow through deteriorated cemented annulus (3), flow through deteriorated cement plugs (4), flow through microannulus between plug and casing (5), and flow through corroded or sheared casing (6). Upward flow is equally possible when $H_2 > H_1$. Not to scale [Wu et al. 2018]..... 4

Figure 2 Relationship between cement core porosity and hydraulic conductivity, and where provided, effective well conductivity, based on data from the studies noted in the legend. Each study is indicated by a different symbol, cement conductivity is shown as solid symbols, effective well conductivity is shown as open symbols, and the age of the wellbore is indicated by the colour of the symbol: < 20 years – black; 20-40 years – blue; > 40 years – red. (Wu et al. 2018). 5

Figure 3 Schematic of aquifer-aquitard system considered for impact assessments using analytical solutions. 7

Figure 4 Leaky wells within an aquitard..... 9

Figure 5 Equivalent hydraulic conductivity of an aquitard with a series of leaky wells as function of well failure density. In the grey shaded area the number of leaky wells/km² ranges from 0.5 to 5. Vertical black line is for one leaky well/km². 10

Figure 6 Relationship between flow through a leaky bore and the effective well hydraulic conductivity (K_{well}) calculated using Equation 13 and parameters shown in Table 2. Dashed lines show the effective well conductivities for a leaky well (0.1 m/d), the example in Figure 5 (100 m/d), and an open well 10^8 (m/d)..... 13

Figure 7 Relationship between flow through a leaky bore and the aquifer hydraulic conductivity calculated using Equation 13 and parameters shown in Table 2. Higher bore hydraulic conductivities may violate the Forchheimer assumption in Darcy’s equation, and require further analysis using turbulent flow equations. The dashed line represents the aquifer hydraulic conductivity used in the analysis. 14

Figure 8 Equivalent hydraulic conductivity of an aquitard with a series of leaky wells ($K_{well} = 0.1$ m/d) as a function of well failure density. 15

Figure 9 Model domain in AlgoMesh indicating the three model layers and grid refinement around the well at the centre of the domain. 16

Figure 10 Time series of groundwater head in layer 1 at the production well and at 10 m, 100 m, 1 km, and 10 km from the production well, scenario 1 – perfectly sealed well. The year 2040 is the start of the post-production phase. 23

Figure 11 Time series of groundwater head in layer 3 at the production well and 10 m, 100 m, 1 km, and 10 km from the production well, scenario 1 – perfectly sealed well.....	23
Figure 12 Time series of groundwater head in layer 1 at the production well and 10 m, 100 m, 1 km, and 10 km from the production well, scenario 2 – leaky well.	24
Figure 13 Time series of groundwater head in layer 3 at the production well and 10 m, 100 m, 1 km, and 10 km from the production well, scenario 2 – leaky well.	24
Figure 14 Time series of groundwater head in layer 1 at the production well and at 10 m, 100 m, 1 km, and 10 km from the production well, scenario 3 – open well.	25
Figure 15 Time series of groundwater head in layer 3 at the production well and 10 m, 100 m, 1 km, and 10 km from the production well, scenario 3 – open well.	26
Figure 16 Groundwater head drawdown cones in layer 1 with delays of between 0 and 1000 years post-production, for the fully sealed well, scenario 1.....	27
Figure 17 Groundwater head drawdown cones in layer 2 (aquitard) with delays of between 0 and 1000 years post-production, for the fully sealed well, scenario 1.	27
Figure 18 Groundwater head drawdown cones in layer 3 (aquifer) with delays of between 0 and 1000 years post-production, for the fully sealed well, scenario 1.....	28
Figure 19 Groundwater head drawdown cones in layer 1 with delays of between 0 and 1000 years post-production, for the leaky well, scenario 2.....	29
Figure 20 Groundwater head drawdown cones in layer 2 with delays of between 0 and 1000 years post-production, for the leaky well, scenario 2.....	29
Figure 21 Groundwater head drawdown cones in layer 3 with delays of between 0 and 1000 years post-production, for the leaky well, scenario 2.....	30
Figure 22 Groundwater head drawdown cones in layer 1 with delays of between 0 and 1000 years post-production, for the open well, scenario 3.....	31
Figure 23 Groundwater head drawdown cones in layer 2 with delays of between 0 and 1000 years post-production, for the open well, scenario 3.....	31
Figure 24 Groundwater head drawdown cones in layer 3 with delays of between 0 and 1000 years post-production, for the open well, scenario 3.....	32

List of Tables

Table 1 Well failure rates with corresponding total well flow area and density of leaky wells. Total number of wells is 425. 10

Table 2 Model parameters sourced from the CDM Smith [2014] Narrabri model. Parameters are defined in the text. 17

Table 3 Effect of mesh size on flow through an abandoned well (scenario 3). 20

Table 4 Comparison between flow through a leaky and fully open well compared with regional flow through the aquitard, using parameters shown in Table 2 and a steady-state model. 21

Table 5 Comparison between flow through a leaky and open well compared with regional flow through the aquitard, for one order of magnitude lower aquitard (Layer 2) K_h and K_v values and a steady state model. Flow through the leaky well is slightly higher in this example because the decreasing aquitard conductivity restricts flow through the aquitard in favour of flow through the well, just as turning off one tap will increase flow slightly through other taps in a multi-tap system. 21

Table 6 Comparison between flow through a leaky and open well compared with regional flow through the aquitard, for one order of magnitude higher aquifer (Layers 1 and 3) K_h and K_v values and a steady state model. 21

Table 7 Summary of metrics for the three well scenarios 34

Executive summary

The project “Bore and well induced inter-aquifer groundwater connectivity: Consequence modelling and experimental design” focuses on identifying the consequences associated with preferential pathways generated by failed or open bore holes in regions where coal seam gas development occurs. The project aims to develop methodologies and techniques that will identify and potentially quantify the potential risks associated with well and bore-induced inter-aquifer connectivity. The project has two components: i) a critical literature review and local-scale assessments using groundwater modelling to identify the types of compromised bore integrity that may be measurable in CSG-bearing basins, and ii) regional groundwater modelling to assess the consequences of well and bore hole connectivity and the number of required connective pathways to create a range of noticeable impacts. This report documents the local-scale assessments that were undertaken to explore whether or not there could be noticeable consequences on the groundwater balance from enhanced inter-aquifer connectivity owing to leakage pathways linked to hydrocarbon wells, groundwater bores, and exploration bores. The local-scale assessments also serves as a test-bed for later regional-scale assessments of potential consequences.

On the basis of a set of analytical solutions this study explores the conditions, both in terms of flow properties of the well seepage pathway and the hydrogeological properties of the aquifers/aquitard system, which may lead to noticeable impacts on the groundwater balance. For this purpose a highly simplified three-layer system is considered comprising of two aquifers separated by an aquitard. A hydrocarbon well or water bore is screened in the deepest aquifer, but has lost its integrity due to casing corrosion or another well failure mechanism. This has resulted in a continuous flow pathway connecting the two previously unconnected aquifers. Two leakage pathways are considered: a leaky well with flow through the cement annulus between the well casing and the rock matrix, which has a moderately high effective well conductivity, and a fully open well or water bore with a very high well conductivity.

Based on the analytical solutions, simple relationships are developed between the density of leaky wells within a specified area of an aquitard and the equivalent hydraulic conductivity of that aquitard. The density of leaky wells provides a proxy for the well failure rate, while the equivalent hydraulic conductivity of the aquitard is a weighted average of the conductivity through the leaky wells and the aquitard. A subsequent set of analytical solutions was developed that identify whether flow through the well is limited by the hydraulic conductivity of the well or the aquifers which provide or accept the flow of water.

A complementary numerical analysis was undertaken using MODFLOW Unstructured Grid model (MODFLOW-USG) with the Continuous Linear Network (CLN) package and MODHMS with the Fracture Well (FWL4) package. Both models are similar in the way they numerically describe the leaky well problem. The results from the numerical models, in terms of flow through leaky wells with different well conductivities, were of the same order of magnitude as flow calculated using the analytical equations, although the analytical equations did not include leakage through an aquitard, nor leakage through an unconfined surficial aquifer.

Based on an analysis of a single well, it is unlikely that there will be an impact from leaky wells on the groundwater balance of a hydrogeological system similar to the Gunnedah Basin (New South Wales), assuming moderately high effective well conductivity. However, it is possible that exploration or repurposed production bores that remain open after the gas production site has been decommissioned will negatively impact the groundwater balance, i.e. groundwater water levels in

the surficial aquifer. Analysis of the cumulative effects of a large number of leaky wells on the regional scale groundwater balance are the subject of future assessments.

Abbreviations

General abbreviations	Description
AHD	Australian height datum
CHB	constant head boundary
CLN	Continuous linear network package from MODFLOW-USG
CSG	Coal seam gas
CSIRO	Commonwealth Scientific and Industrial Research Organisation
MODFLOW-USG	MODFLOW-Unstructured Grid
MODHMS-FWL4	MODHMS fracture well package
US EPA	United States Environmental Protection Agency

Glossary

Term	Description
Abandoning	To cease efforts to produce fluids from a well and to plug the well without adversely affecting the environment.
Annulus	The gap between tubing and casing or between two casing strings or between the casing and the wellbore. The annulus between the tubing and casing is the primary path for producing gas from CSG wells.
Bore	A narrow, artificially constructed hole or cavity used to intercept, collect or store water from an aquifer, or to passively observe or collect groundwater information. Also known as a borehole or drill hole. This report uses the term 'bore' in reference to the extraction, exploration or monitoring of water.
Borehole	A hole drilled for purposes other than production of oil, gas or water (e.g. a mineral exploration borehole).
Coal seam gas	A form of natural gas (generally 95 to 97% pure methane, CH ₄) typically extracted from permeable coal seams at depths of 300 to 1000 m. Also called coal seam methane (CSM) or coalbed methane (CBM).
Decommissioning	The process to remove a well from service.
Effective well hydraulic conductivity	The hydraulic conductivity that can be used in an equation or model to represent the conductivity of the pathway from one formation to another through a well. The conductivity may be a result of flow through any or a number of the pathways as indicated in Figure 1.
Equivalent conductivity	The regional vertical conductivity of the aquitard/leaky well system, defined as an average of hydraulic conductivities of the aquitard and the leaky wells, weighted by the areas of leaky wells and total production zone.
Formation pore pressure	The fluid pressure in the porous rock around the well.
Hydraulic fracturing	Also known as 'fracking', 'fraccing', 'fracture simulation' or 'fluid-driven fractures', is the process by which hydrocarbon (oil and gas) bearing geological formations are 'stimulated' to enhance the flow of hydrocarbons and other fluids towards the well. The process involves the injection of fluids, gas, proppant and other additives under high pressure into a geological formation to create fractures connecting the well to the reservoir. The fracture acts as a high conductivity channel through which the gas, and any associated water, can flow.
Hydrostatic pressure	The theoretical pore pressure that would be expected purely from the weight of water in a column running from the depth of interest to the surface.
Open well	As used in this report: A completed well or wellbore that has continuity through the well column and open communication with the aquifer. Examples include an abandoned exploration wellbore that has not been through a process of decommissioning or a production well that has been repurposed for water extraction.
Offset wellbore	An existing wellbore close to a proposed well that provides information for planning the proposed well.
Well	As used in this report: a completed structure, following drilling of a wellbore, used for production of oil or gas and typically including casing, cement, and tubing strings.
Well failure (1)	All well barriers failing in sequence and a leakage pathway being created across all the well barriers (King and King 2013).
Well failure (2)	Well failure or loss of well integrity may result from a well breach (or number of well breaches).

Term	Description
	Well failure can take the form of a hydrological breach (fluid movement between different geological units) or environmental breach (fluid leaks from the well at surface or contamination of water resources).
Wellbore	The hole initially produced by drilling and intended to be cased and cemented to create a well for production of oil or gas.

Symbols

Symbol	Short description, units
A	Cross-section flow area [m ²]
A_{ref}	Area of the reference aquitard [m ²]
$A_{well, i}$	Cross sectional area of each leaky well [m ²]
d	Cylinder length [m]
D	Hydraulic diameter of conduit [m]
G	Acceleration of gravity [m ⁻²]
h	Hydraulic head [m]
h_f	Head loss due to friction [m]
k	Permeability [m ²]
K_h	Horizontal hydraulic conductivity [m.d ⁻¹]
K_{eq}	Equivalent hydraulic conductivity of the combined aquitard and the leaky wells [m/d]
K_{ref}	Background hydraulic conductivity for aquitards [m.d ⁻¹]
K_v	Vertical hydraulic conductivity [m.d ⁻¹]
K_{well}	Effective hydraulic conductivity of the well [m.d ⁻¹]
L	Length of flow path [m]
Q	Volumetric fluid flux [m ³ .d ⁻¹]
r_w	Well radius [m]
ρ	Density of failed wells [m ² /m ²]
S_y	Specific yield [-]
S_s	specific storage [m ⁻¹]
T_1, T_2	Transmissivity for Aquifer-1, -2 [m ² /d]
z	Thickness of the aquitard [m]

1 Introduction

Most literature related to impacts from coal seam gas or shale gas production centres around the impact of hydraulic fracturing on drinking water quality and the leakage of methane gas to surficial aquifers or to the land surface [Vengosh et al., 2014]. Well failure has been identified as a possible pathway for migration of such contaminants from the hydrocarbon reservoir to shallower aquifers. Reagan et al. [2015] identified four broad classes of plausible failure scenarios for upward migration of contaminants associated with hydraulic fracturing, which included (i) fractures from the stimulation operation intercept older abandoned unplugged wells (e.g. conventional oil and gas wells), and (ii) continuous and highly permeable pathways via poorly completed wells due to inadequate design, installation or weak cement. In a review of well integrity across the conventional and unconventional gas industry in the US, Jackson [2014] illustrates the severity of well integrity failure, especially in Pennsylvania where since 2005 the Department of Environmental Protection has confirmed more than 100 cases of well-related groundwater contamination. According to Jackson [2014], well integrity is the key to minimizing many of the risks associated with hydraulic fracturing and unconventional resource extraction. Finally, Jackson [2014] identifies the need for much more information on the structural integrity of older producing wells and abandoned wells.

Dusseault and Jackson [2014] investigated the possibility of hydraulic fracturing fluids moving upwards to shallow groundwater. By considering several factors that inhibit uncontrolled upward migration of induced fractures, Dusseault and Jackson [2014] conclude that the migration of hydraulic fracturing or formation fluids (including natural gas) to the surface as a result of deep hydraulic fracturing of typical shale-gas reservoirs appears most unlikely. They do recognise, however, that the real subsurface threat to shallow groundwater contamination is likely related to a combination of factors involving the characteristics of annular cement seals of production wells and the presence of natural gas in intermediate zones between shallow aquifers and the target shale-gas formations. Dusseault and Jackson [2014] recognise that the seepage pathways presenting greatest risk of hydraulic fracture fluid migration are those associated with decommissioned wells intersecting the hydraulic fracturing volume. Indeed, the most serious fluid communication risk during hydraulic fracturing is the possible intersection of the fractured zone with offset wellbores (e.g. old production gas wells) that pass through the stimulated rock volume created by the hydraulic fractures. If the quality of the cement and completion of such offset wells is poor, fracturing fluids that moved laterally to the offset vertical cased wells could then feasibly move upward along the annulus between the casing and the rock. Examples of inter-wellbore communication have been reported for the Barnett Shale of Texas (approximately 200 m distance between wells), Alberta (maximum distance up to 2400 m), and British Columbia (communication reported up to 4100 m distance).

In CO₂ sequestration research concerns are usually around the containment capacity of the cap rock which controls loss of CO₂, rather than migration of water potentially causing drinking water quality issues [Lewicki et al., 2007; Nordbotten et al., 2008]. Few studies have considered the impacts of inter-aquifer leakage on groundwater flow and the groundwater balance due to seepage pathways caused by unconventional gas wells, conventional oil and gas wells re-purposed for groundwater extraction, water bores, decommissioned wells, or exploration bores.

Studies that have undertaken numerical modelling of groundwater flow through seepage pathways caused by well integrity failure, usually resort to dual-phase models (water-gas), such as Eclipse [Schlumberger, 2011], DuMu^x [Flemisch et al., 2011], or TOUGH+RealGasH₂O simulator [Moridis and Freeman, 2014]. Of the few numerical modelling studies discussed in this report, the focus was always on changes to groundwater quality, not groundwater balance or heads. Using numerical

simulation models Kissinger et al. [2013] tested under what circumstances several hypothesized flow paths for fracturing fluid, brine and methane would result in leakage of such fluids into shallower layers. The simulations used literature-based parameterisation (upper and lower bounds of hydraulic parameters) for potential hydraulic fracturing sites in Germany (North Rhine-Westphalia and Lower Saxony). In the study by Nowamooz et al. [2015], methane and formation fluid leakage was modelled along the casing of a decommissioned shale gas well. Reagan et al. [2015] carried out numerical simulations of water and gas transport between a shallow tight-gas reservoir (characterised by an ultralow permeability in the range of a nano-Darcy) and a shallower freshwater aquifer following hydraulic fracturing operations. Two general failure scenarios were considered in the simulations: connection between the reservoir and aquifer is assumed to occur (i) via a fracture or fault and (ii) via a deteriorated, pre-existing nearby well.

Estimates of drawdown caused by depressurising coal layers may be obtained using single phase models, but this is known to overestimate impact (i.e. conservative) compared with dual-phase models [Moore et al., 2014]. Single phase models such as MODFLOW 2005 [Harbaugh, 2005] do not represent the process of pore water displacement by gas, and therefore do not account for the reduction of permeability due to the presence of another (gas) phase which makes the coal seam unsaturated with respect to water. In other words, under dual-phase flow conditions, effective relative permeabilities need to be defined for both the water and gas phase. The effective permeability is a measure of the permeability of a porous medium for one fluid phase when the medium is saturated with more than one fluid.

For a dual-phase flow system, typically in the near vicinity of the coal seam gas extraction areas, a simplified representation of the multi-phase process by a single-phase model may yield results which are erroneous, but on the conservative side in terms of drawdown prediction. Despite the lack of this predictive accuracy, the single-phase flow model may still be fit-for-purpose when regional scale screening of potential impacts of well integrity failure is being undertaken. More detailed assessments with a dual-phase model can then be undertaken to confirm or refute the degree of impact identified by the regional-scale single-phase model. Furthermore, regional-scale implementation of a dual-phase flow model across potentially hundreds or thousands of wells is computationally very demanding [Moore et al., 2014]. The primary advantage of single phase models is their relatively lower computational requirements (and therefore short solution calculation times) in comparison to multi-phase models. This is of particular benefit to models featuring large spatial extents and/or long hydraulic equilibration times. Furthermore, single-phase models are useful for initial estimates of unconventional gas impacts on hydrogeology, particularly as a fast, reliable analysis to flag regions that require modelling in more detail.

This report outlines the development of a single-phase numerical groundwater flow model of a single, leaky CSG well to explore the parametric space under which measurable changes to the groundwater balance and heads can occur. The single-well evaluation reported here is a precursor to a future regional-scale application in which the cumulative effects of several hundred leaky CSG wells will be evaluated. The research was also intended to determine (i) whether the available numerical implementations in MODFLOW of seepage pathways via leaky wells are suitable for modelling this type of problem, (ii) what an acceptable spatial discretisation around the wells would be for future implementation in the regional model, and (iii) the validity of the numerical models against analytical solutions.

Several hydrologic metrics for detecting change to a groundwater system due to enhanced inter-aquifer connectivity have been considered. At the local scale, the first metric determines the relative contribution to inter-aquifer groundwater exchange from leaky, abandoned or repurposed CSG wells versus flow through aquitards for a parameter space relevant to Australian sedimentary coal basins. The second metric determines the sensitivity of aquifer recovery time in the post-production phase to various hydrogeological parameters. The third metric quantifies the (maximum) head changes during or after the gas extraction phase.

2 Conceptualisation of leaky wells

2.1 Seepage pathway conceptualisation

In a recent review of national and international literature on bore and well induced inter-aquifer connectivity, Wu et al. [2018] summarised well failure mechanisms and developed several conceptualisations of plausible hydrocarbon reservoir-aquifer failure pathways. Four major pathways - and their conceptualisations - for movement of water between strata were identified: (i) pathways linked to uncased exploration bores, (ii) pathways linked to decommissioned production wells, (iii) pathways linked to oil and gas wells repurposed for water extraction and water bores with degraded casing, and (iv) natural pathways linked to fractures and faults between wellbores and surficial aquifers. For the purpose of this study, one representative conceptualisation will be taken forward to (i) test the suitability of available numerical implementations in MODFLOW of seepage pathways via leaky wells, (ii) explore the effect of spatial discretisation on metrics of change, and (iii) compare the numerical models with analytical solutions.

The conceptualisation for pathways linked to decommissioned production wells is selected for the purpose of this study. In decommissioned and abandoned wells, loss of integrity may lead to the following pathways for water migration [Wu et al., 2018] (Figure 1):

- through a microannulus between the cement casing and the soil/rock matrix (1) or the steel well casing (2)
- through a deteriorated cement sheath between the well casing and soil/rock matrix (3)
- through deteriorated cement plugs used in decommissioning (4, 5), and
- through the well itself, via corrosion holes, shear or tensile damage (6).

In Figure 1 flow is from upper aquifer to lower aquifer based on the downward head gradient ($H_1 > H_2$). This scenario represents the period of depressurisation during or long after gas extraction has ended (note that recovery to the initial hydraulic head condition in the coal seam formation may take hundreds of years [Wu et al., 2018]). When an upward gradient exists ($H_2 > H_1 + h$, where h is the height of aquifer 2 above aquifer 1), flow will be from the lower to the upper aquifer. The latter condition was observed both pre-CSG and post-CSG extraction in several locations of a regional groundwater model that provided realistic head boundary conditions for the current study [Wu et al., 2018]. Although this scenario involves a gas-saturated hydrocarbon reservoir, with a gradually decreasing gas phase as the reservoir re-saturates, it is conceptualised here as single-phase water-saturated system to allow use of a single-phase groundwater flow model. It has been demonstrated that conceptualisation of groundwater flow problems associated with CSG production using single-phase models will over predict drawdown, as higher pressures are required to remove water from rock matrix where gas replacement is not modelled [Moore et al., 2014]. For this reason, the drawdown results from the single-phase groundwater flow modelling presented in this report are likely conservative. If the predicted impact is significant, a multi-phase flow modelling approach may be necessary for a more exact quantification.

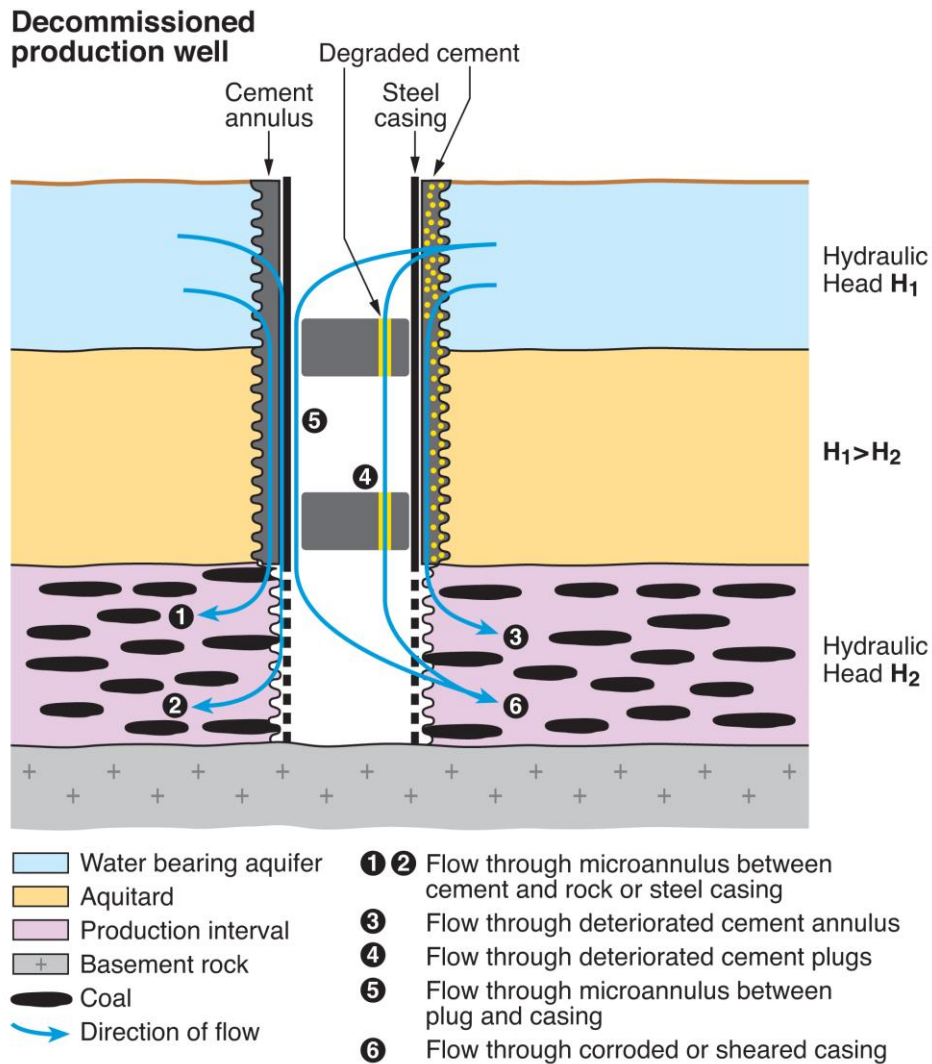


Figure 1 Pathways for water movement in cemented wellbores: flow through microannulus between cement and rock matrix (1) or steel casing (2), flow through deteriorated cemented annulus (3), flow through deteriorated cement plugs (4), flow through microannulus between plug and casing (5), and flow through corroded or sheared casing (6). Upward flow is equally possible when $H_2 > H_1$. Not to scale [Wu et al. 2018].

For a single leaky well, single-phase flow through the well may be represented using the Darcy flow equation with an effective well hydraulic conductivity. The flow through the well will be governed by the effective hydraulic conductivity, the radius of the bore hole and the head difference between the top and bottom of the well. Where the effective bore conductivity is high, flow through the bore may be limited by the transmissivity of the alluvial aquifer and the production zone (see discussion in Section 2.2). This was demonstrated by Silliman and Higgins [1990] for a simplified hydrogeological system with two aquifers separated by an aquitard. When the well conductivity is high relative to aquifer transmissivity, the aquifers can limit radial flow to or from the well location.

2.2 Well hydraulic properties

To use a single-phase groundwater flow model to estimate leakage through a well, accurate information is required on the head gradient between the connected aquifer(s) and hydrocarbon production zone and on the effective well hydraulic conductivity. There are currently no known estimates of effective hydraulic conductivity for the degraded cement of a well annulus available for Australian conditions. However, as part of research into integrity of wellbore cement in CO₂ storage wells, Connell et al. [2014] carried out experimental and geochemical simulation studies on cement degradation under conditions that reflect the cement-formation interface within a reservoir. Although the effect of cement degradation on permeability was not quantified, the hypothetical scenarios illustrated the potential degradation rates and timeframes involved and summarised the sequence of conditions that could lead to cement degradation.

Surveys of field and laboratory measured cement hydraulic conductivity and effective well hydraulic conductivity in the US have been reported in Carey et al. [2007], Crow et al. [2010], Duguid et al. [2013] and Hawkes and Gardner [2013]. These data are summarised in Figure 2. Note that the term permeability is used by reservoir engineers, while hydraulic conductivity is more commonly used by hydrogeologists. On average, there was a four order of magnitude difference between the cement conductivity and effective well conductivity. Effective well hydraulic conductivity depends on whether the flow is through the cement annulus or within the well itself, the type of cement used and its condition. Cement condition is a function of the age of the well and the chemical reactivity of the in-situ water in contact with the cement.

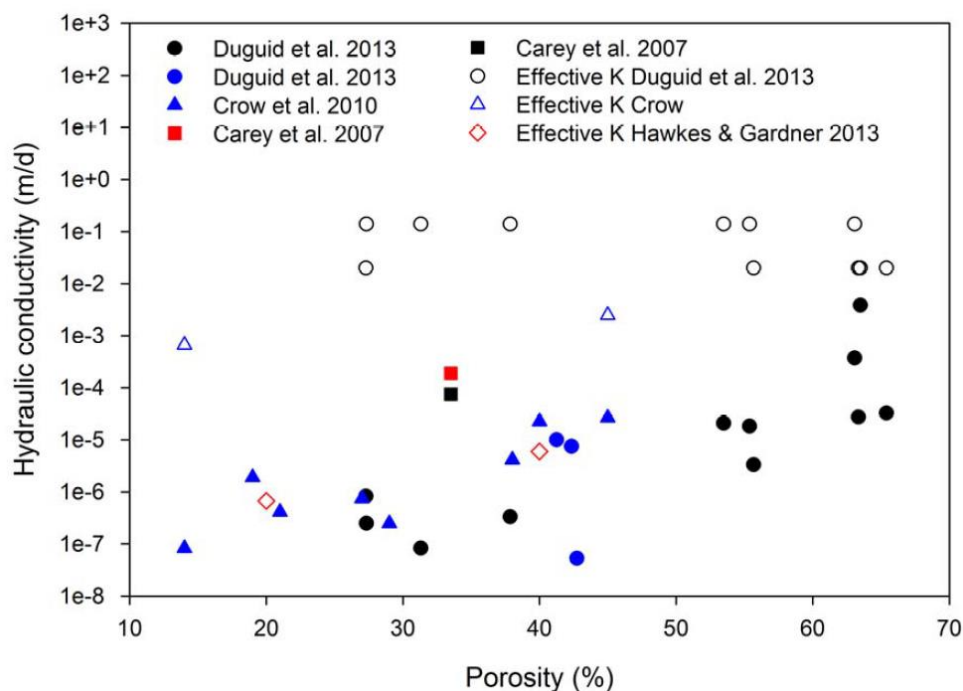


Figure 2 Relationship between cement core porosity and hydraulic conductivity, and where provided, effective well conductivity, based on data from the studies noted in the legend. Each study is indicated by a different symbol, cement conductivity is shown as solid symbols, effective well conductivity is shown as open symbols, and the age of the wellbore is indicated by the colour of the symbol: < 20 years – black; 20-40 years – blue; > 40 years – red. (Wu et al. 2018).

Effective well conductivities have been used in some numerical studies. For instance, Nordbotten et al. [2009] used an effective well conductivity of 7.42×10^{-2} m/d (8.6×10^{-7} m/s) or 100 mD (milliDarcy). As part of a broader US EPA study [US EPA, 2015] on the relationship between hydraulic fracturing

and drinking water quality, Reagan et al. [2015] carried out numerical simulations of water and gas transport between a shallow tight-gas reservoir (characterised by an ultralow permeability in the range of a nano-Darcy) and a shallower freshwater aquifer following hydraulic fracturing operations. The failed well behaviour was investigated for the following cement permeabilities: $k=10^{-9} \text{ m}^2$, $k=10^{-12} \text{ m}^2$, $k=10^{-15} \text{ m}^2$ and $k=10^{-18} \text{ m}^2$ (1000 D, 1 D, 1 mD, and 1 μD , respectively).

2.3 Well hydraulic gradient

The head difference between a water bearing aquifer and underlying hydrocarbon reservoir varies depending on the specific hydrogeological conditions for the site. This was recently substantiated using the numerical groundwater model for the proposed Narrabri CSG production area in New South Wales, Australia, where Wu et al. [2018] identified spatially varying, pre-production head differences of between 49 m downward and 25 m upward over a vertical distance of around 800 m between water bearing aquifers and the CSG reservoir. After gas production ceased, the head differences further increased and reached a maximum of up to 115 m, with flow in the downward direction. These head differences across various low-permeable formations were used here to develop a generic, yet realistic numerical model of a leaky single-well.

2.4 Exploring the potential impact space with analytical solutions

On the basis of a set of analytical solutions we explore the conditions, both in terms of flow properties of the seepage pathway and the hydrogeological properties of the aquifers/aquitard system, which may lead to noticeable impacts on the groundwater balance. For this purpose a highly simplified three-layer system is considered comprising two aquifers separated by an aquitard (Figure 3). A hydrocarbon well or water bore is screened in the deepest aquifer, but has lost its integrity due to casing corrosion or other well failure mechanisms [Wu et al. 2018]). This has resulted in a continuous flow pathway effectively connecting the two previously non-connected aquifers.

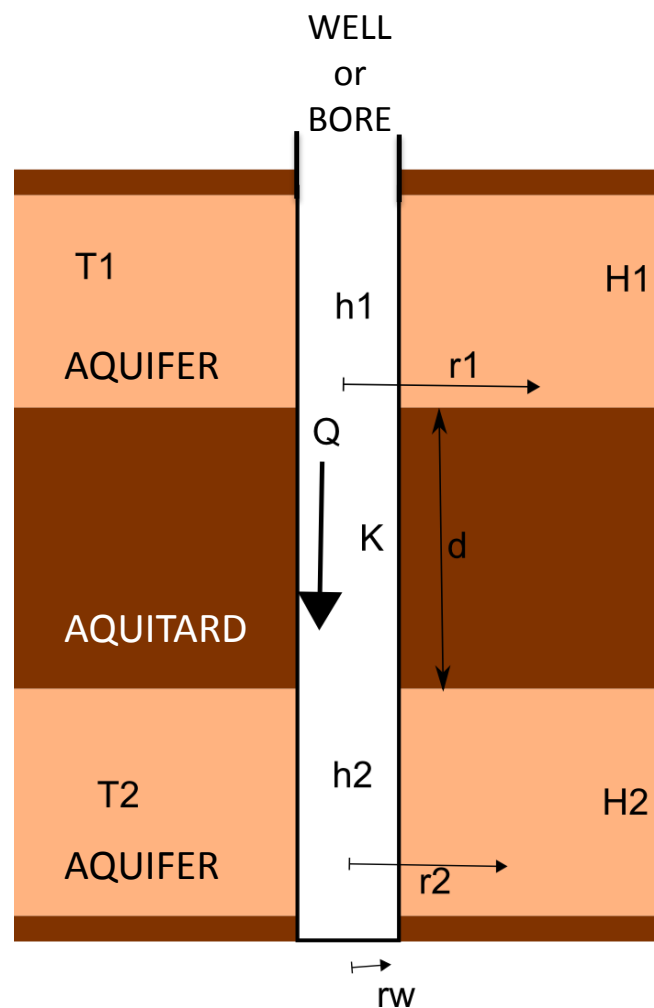


Figure 3 Schematic of aquifer-aquitard system considered for impact assessments using analytical solutions.

Although the aquifers are considered to be non-connected, there generally is some very small diffuse migration of water through the aquitard, e.g. from the upper to lower aquifers based on the hydraulic gradient conditions of Figure 3. Whether or not a leaky well will have an impact on the regional groundwater system depends on whether this diffuse flow rate has perceptibly increased. This can be assessed by comparing the vertical hydraulic conductivity of a number of leaky wells within a production area with the vertical hydraulic conductivity of the aquitard over the same area.

We first develop a simple relationship between the density of leaky wells within a specified area of an aquitard – as a proxy for well failure rate – and the equivalent hydraulic conductivity of the combined aquitard / leaky bore population which accounts for the combined flow through leaky

wells and aquitard. We subsequently develop a set of analytical solutions that identify for which hydrogeological conditions flow through leaky wells, required to significantly increase the equivalent conductivity of the aquitard, is physically possible.

Consider an aquitard where A_{ref} (m^2) is the area of the reference aquitard considered in the analysis; the aquitard hosts both a number of intact and leaky well or bores (Figure 4). The cross sectional area of each leaky well i is $A_{well,i}$ (m^2). The density of failed wells, ρ , is defined as:

$$\rho = \frac{1}{A_{ref}} \sum_{i=0}^n A_{well,i} \quad \text{Equation 1}$$

The flux Q (m^3/d) across the aquitard reference area A_{ref} is calculated using Darcy's Law:

$$Q = K_{eq} A_{ref} \frac{dh}{dz} \quad \text{Equation 2}$$

where K_{eq} (m/d) is the equivalent hydraulic conductivity of the combined aquitard and the leaky wells, ∂h (m) is the head difference between the aquifers and ∂z (m) is the vertical separation distance between the two aquifers, i.e. the thickness of the aquitard. Q is also equal to the sum of the flow through the aquitard, Q_{ref} (m^3/d), and flow through the leaky bores Q_{well} (m^3/d):

$$Q = Q_{ref} + Q_{well} = ((1 - \rho)K_{ref} + \rho K_{well}) A_{ref} \frac{dh}{dz} \quad \text{Equation 3}$$

The equivalent hydraulic conductivity K_{eq} is calculated from the conductivity of the aquitard, K_{ref} (m/d), and the wells, K_{well} (m/d):

$$K_{eq} = (1 - \rho)K_{ref} + \rho K_{well} \quad \text{Equation 4}$$

It is then possible to define the density ρ of leaky wells, i.e. the surface area of all leaky wells relative to the flow area through the aquitard in terms of K_{eq} and K_{ref} .

Assuming the density of leaky wells (A_{well}/A_{ref}) is very small ($<10^{-5}$), or $\rho < 1$, then

$$K_{eq} = K_{ref} + \rho K_{well} \quad \text{Equation 5}$$

We define K_{eq} to be significantly different from K_{ref} , i.e. $K_{eq} > 2 K_{ref}$, therefore:

$$2K_{ref} < K_{ref} + \rho K_{well} \quad \text{Equation 6}$$

$$K_{ref} < \rho K_{well} \quad \text{Equation 7}$$

which finally yields an alternative expression for the density of failed wells, ρ :

$$\rho > \frac{K_{ref}}{K_{well}} \quad \text{Equation 8}$$

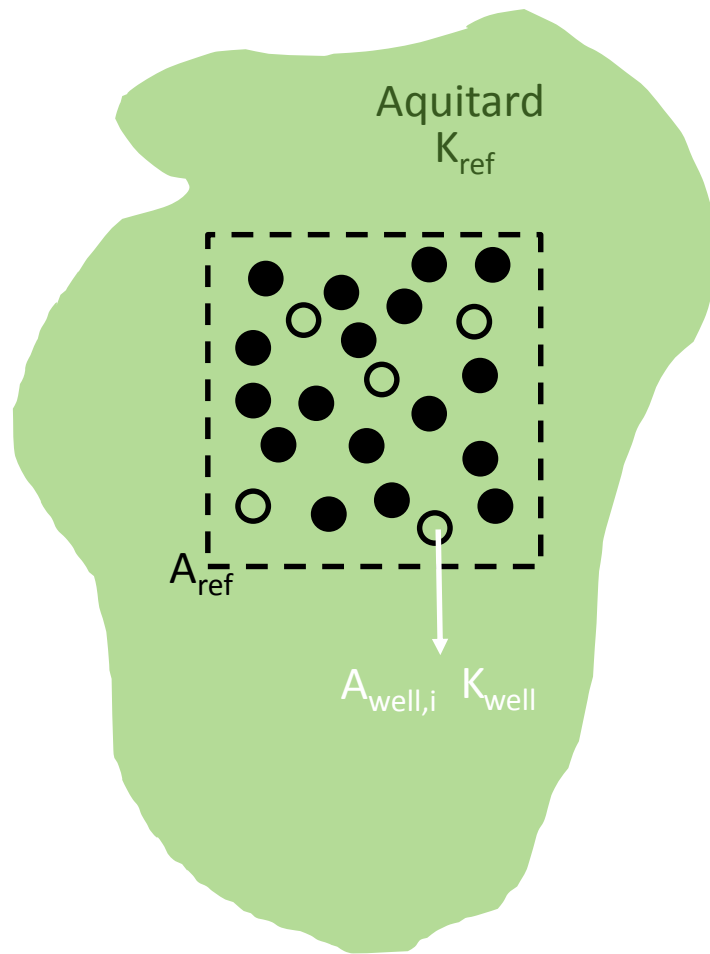


Figure 4 Leaky wells within an aquitard.

To illustrate the significance of Equation 8, consider an aquitard with $K_{ref} = 10^{-4}$ m/d and a series of leaky wells with $K_{well} = 100$ m/d (representing a value between open well flow and flow through a degraded cement annulus), such that the density of leaky wells $\rho = K_{ref} / K_{well} = 10^{-6}$. This is equivalent to five leaky wells with a total flow area of 1 m^2 (well radius of 0.25 m or 0.2 m^2 flow area per well; a similarly large radius of 0.2 m was used by Nordbotten et al. 2009) per km^2 of aquitard. The dependency of K_{eq} for the combined aquitard-leaky well system on the density of leaky wells is illustrated in Figure 5. The value of K_{eq} becomes significantly larger than K_{ref} (background conductivity of an aquitard without leaky wells) once ρ exceeds approximately 10^{-6} . At this point K_{eq} exceeds K_{ref} by about 10%. For the remainder of the discussion, this condition is considered to represent the case where K_{eq} is 'significantly different' from K_{ref} .

Consider now a gas production area which consists of 425 CSG wells on an area of 425 km^2 , i.e. one well per km^2 . The density of leaky wells is calculated for well failure rates of 1, 5, 10, 50 and 100%, assuming again 0.2 m^2 flow area per leaky well (Table 1). Calculated values of ρ range from 0.02×10^{-7} to 2×10^{-7} , which demonstrates that for these conditions the equivalent hydraulic conductivity of the combined aquitard-leaky well system would not become significantly different from the aquitard background K_{ref} of 10^{-4} m/d or $\sim 10^{-9}$ m/s. In other words, at a density of one leaky well per km^2 the flow through the aquitard, however low, would not be significantly influenced by the additional flow through the leaky well. Based on Figure 5 and Table 1, a five times higher well density of 5 wells/ km^2 would be required to create a situation that would significantly alter K_{eq} resulting in significant increase (i.e. 10% above background) in flux across the combined aquitard-leaky well system. Such a

high CSG well density is not common in the active CSG production areas in Queensland and New South Wales; a CSG well density of approximately 1 per km² is the standard.

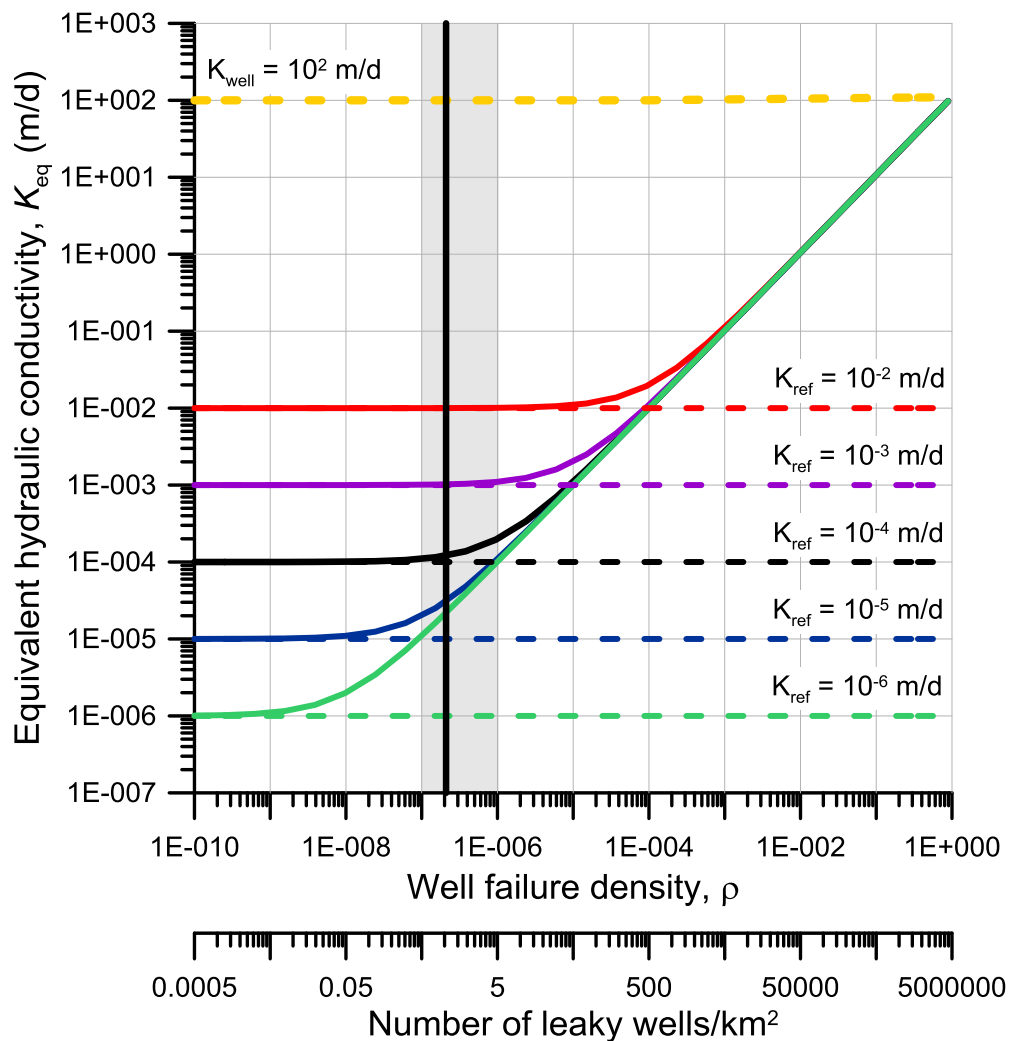


Figure 5 Equivalent hydraulic conductivity of an aquitard with a series of leaky wells as function of well failure density. In the grey shaded area the number of leaky wells/km² ranges from 0.5 to 5. Vertical black line is for one leaky well/km².

Table 1 Well failure rates with corresponding total well flow area and density of leaky wells. Total number of wells is 425.

Well failure rate (%)	Well flow area, A_{well} (m ²)	Density, ρ (-)
1	0.85	0.02×10^{-7}
5	4.25	0.1×10^{-7}
10	8.5	0.2×10^{-7}
50	42.5	1×10^{-7}
100	85	2×10^{-7}

The above analysis is now repeated for both higher and lower values of K_{ref} , i.e. for $K_{ref} = 10^{-3}$ and 10^{-2} m/d (or $\sim 10^{-8}$ to 10^{-7} m/s) and $K_{ref} = 10^{-5}$ and 10^{-6} m/d (or $\sim 10^{-10}$ to 10^{-11} m/s). The corresponding dependencies of K_{ref} on the density of leaky wells is shown in Figure 5. As the background hydraulic conductivity of the aquitard increases, the less sensitive it becomes to additional flow pathways through leaky wells. Indeed, for $K_{ref} = 10^{-3}$ and 10^{-2} m/d the aquitard would need to be punctured by at least 5 to 50 leaky wells, respectively, to obtain values for K_{eq} exceeding the background value by 10% or more. However, for lower background hydraulic conductivities K_{ref} of 10^{-5} and 10^{-6} m/d, the aquitard becomes increasingly more sensitive such that a density of 0.05 to 0.005 leaky wells/km² would suffice to increase K_{eq} above its background value by 10% or more. Because aquitards easily have hydraulic conductivities less than 10^{-5} and 10^{-6} m/d, there is a need to investigate if the assumed hydraulic conductivity of 100 m/d, or any other high value for that matter, is physically plausible for typical hydrogeological – and thus flow – conditions within sedimentary aquifers and coal formations.

The subsequent analysis is about determining the hydrological parameter space for which the conditions identified in the previous analysis are possible. Whether or not flow through leaky wells or bores will have an impact on the water balance of an aquifer (e.g. aquifer 1 in Figure 3), will depend on whether such flow is controlled by the effective hydraulic conductivity of the well or bore (K_{well}) or whether it is controlled by the transmissivities of the aquifers. When it is controlled by the transmissivity of the aquifers, whatever the value of K_{well} (low to very low without loss of integrity or high to very high if fully degraded), the flow through the wells will not be sensitive to the degree of well integrity, and to a certain degree, the cumulative flux through many wells will also not be sensitive to the number of wells. If the flow is controlled by the effective well conductivity, the flow is sensitive to the value of K_{well} , and the cumulative flux depends on the number of wells that have lost integrity. By using a set of analytical solutions we will define more precisely under which hydrogeological and well conditions flows through wells or bores are considered important enough to alter the groundwater balance.

The system of equations considered in this analysis is developed as follows. First of all, assume flow into the well in the top aquifer (aquifer-1), Q_1 , can be represented by the Thiem equation [Silliman and Higgins, [1990]. The Thiem equation assumes that the system is at equilibrium, the pumping well and observation wells are only screened in tested aquifer and are fully penetrating, and that the aquifer is fully confined:

$$Q_1 = \frac{2\pi T_1(H_1 - h_1)}{\log\left(\frac{r_1}{r_w}\right)} \quad \text{Equation 9}$$

where T_1 is transmissivity (m²/d) for Aquifer-1, H_1 is hydraulic head (m) in aquifer-1 at radial distance r_1 (m), and h_1 (m) is the head at well radius r_w (m). Similarly, flow into aquifer 2 from the well, Q_2 , can be represented in the same way:

$$-Q_2 = \frac{2\pi T_2(H_2 - h_2)}{\log\left(\frac{r_2}{r_w}\right)} \quad \text{Equation 10}$$

where T_2 is transmissivity (m²/d) for Aquifer-2, H_2 is hydraulic head (m) in aquifer-2 at radial distance r_2 (m), and h_2 (m) is the head at radial distance r_w (m). Finally, the potential flow through the leaky well Q_{well} (m³/d) is described as flow through a cylinder with radius r_w (m), length d (m) and effective hydraulic conductivity K_{well} (m/d), and is expressed as (from Darcy's Law):

$$Q_{well} = \frac{\pi K_{well}}{d} r_w^2 (h_1 - h_2) \quad \text{Equation 11}$$

where h_1 and h_2 are the hydraulic head (m) at the entry (top aquifer) and exit (bottom aquifer) point of the leakage pathway. When the system is in equilibrium, the flow rates into the well, through the well and out of the well are equal.

$$Q_{well} = Q_1 = Q_2 = Q \quad \text{Equation 12}$$

This system of three equations with three unknowns, h_1 , h_2 and Q is solved for flow through the borehole as follows:

$$Q = \frac{2\pi^2 K_{well} T_1 T_2 r_w^2 (H_1 - H_2)}{\pi K_{well} T_1 r_w^2 \log\left(\frac{r_2}{r_w}\right) + \pi K_{well} T_2 r_w^2 \log\left(\frac{r_1}{r_w}\right) + 2T_1 T_2 d} \quad \text{Equation 13}$$

Flow through the well was calculated for different values of the head difference between aquifers 1 and 2, the effective well conductivity, K_{well} , and aquifer transmissivity (T_1 and T_2). Using Equation 13, it is possible to determine when the flow through the well is controlled by the well hydraulic conductivity, or by the aquifer transmissivity. Where the flow is controlled by the conductivity of the well, the density of the leaky wells will determine the impact on the aquifers. If, on the other hand, flow through the leaky well is controlled by the aquifer transmissivity, the density of leaky wells will be less important (see further).

Based on Equation 13, for any given head difference between the two aquifers $H_1 - H_2$, flow through the leaky well, Q , is controlled by the minimum of K_{well} , T_1 or T_2 . From Equation 11,

$$Q \leq \frac{\pi K_{well} r_w^2}{d} (H_1 - H_2) \quad \text{Equation 14}$$

When flow through the well is controlled by the aquifer's transmissivity T_1 or T_2 , Q will be considerably less than the potential flow through the well, Q_{well} . Here 'considerably less' is defined as at least one tenth of the potential flow:

$$Q < 0.1 Q_{well} \quad \text{Equation 15}$$

By solving for K_{well} in Equations 11, 12, 13 and 14 it is possible to derive the range of K_{well} values for which flow is no longer controlled by the hydraulic conductivity of the leaky well or bore, but controlled by the aquifer transmissivities T_1 and T_2 :

$$K_{well} \geq \frac{5.7 T_1 T_2 d}{r_w^2 \left(T_1 \log\left(\frac{r_2}{r_w}\right) + T_2 \log\left(\frac{r_1}{r_w}\right) \right)} \quad \text{Equation 16}$$

If it is assumed that aquifer 1 is a thick weathered or alluvial aquifer, Equation 16 can be simplified by defining the transmissivity of the production zone (here aquifer 2) to be significantly lower than the water bearing aquifer (aquifer 1). Similarly, r_1 and r_2 , the distances from the leaky bore where head drop is considered negligible, are likely to be greater than ten times the bore radius and less than 1000 times the bore radius where hydrogeological properties would be different from T_1 and T_2 and thus invalidate use of a simple equation like Equation 19 which assumes heterogeneous aquifers. By assuming that:

$$T_1 \gg T_2 \quad \text{Equation 17}$$

and

$$10r_w < r_2 < 1000r_w \quad \text{Equation 18}$$

Equation 13 can then be simplified to:

$$K_{well} \geq \frac{1.9T_2d}{r_w^2} \quad \text{Equation 19}$$

Equation 19 defines the values of K_{well} for which flow through the well or bore is not limited by its hydraulic conductivity, but by the transmissivity of aquifer 2, i.e. T_2 . Under such conditions, the aquifer transmissivity makes the density of leaky wells less important.

Continuing the example problem from this section, we will include the effects of the aquifer transmissivity on flow through the well. Equation 13 was evaluated for an aquifer system based on the proposed CSG development area in the Narrabri groundwater model [CDM Smith 2014]. The example had a 114 m thick surficial aquifer, 600 m thick series of aquitards and 21 m thick production interval and head difference of 100 m between surficial aquifer and production interval, as described in Section 3 below. Flow through the well was calculated for a range of effective well conductivities (assuming open communication with the aquifer):

- K_{well} from 10^{-4} m/d to 10^8 m/d, with a fixed aquifer conductivity of 0.1 m/d, and
- K_{well} of 10^8 m/d (representing a fully open flowing well), 100 m/d (the well conductivity from Figure 5) and 0.1 m/d (well leaking through the degraded cement annulus), for a range of aquifer conductivities of 10^{-4} m/d to 10^8 m/d.

As shown in Figure 6, flow through the leaky well, Q , is linearly related to the head difference between the water producing aquifer and the production zone for a realistic range of well effective hydraulic conductivity, K_{well} . Flow, Q , is logarithmically related to K_{well} while K_{well} is low, then limited by the aquifer transmissivity (aquifer $K = 0.1$ m/d) to a constant flow rate when K_{well} is high (Figure 6). Flow through the well is limited by the aquifer K when K_{well} is greater than 10^4 m/d.

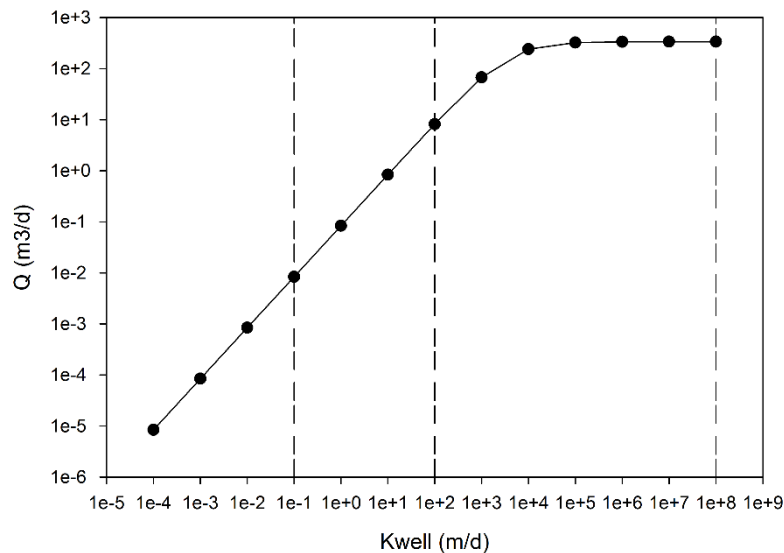


Figure 6 Relationship between flow through a leaky bore and the effective well hydraulic conductivity (K_{well}) calculated using Equation 13 and parameters shown in Table 2. Dashed lines show the effective well conductivities for a leaky well (0.1 m/d), the example in Figure 5 (100 m/d), and an open well 10^8 (m/d).

For the example shown in Figure 5, flow through the well (with $K_{well} = 100$ m/d) will be limited by aquifer conductivity when it is less than 0.1 m/d (Figure 7, dashed line). The latter conductivity is a

realistic condition for many groundwater aquifers; considering this parameter combination, flow through the well may be limited by either aquifer or well effective conductivity. As a result, bore density is an important parameter to consider when assessments are being made about the potential impact of leaky wells on equivalent conductivity of aquitards, and thus on the groundwater balance.

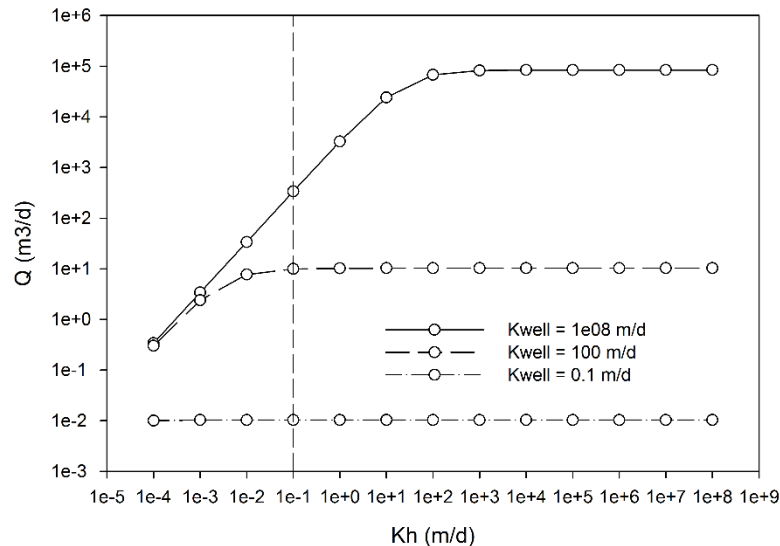


Figure 7 Relationship between flow through a leaky bore and the aquifer hydraulic conductivity calculated using Equation 13 and parameters shown in Table 2. Higher bore hydraulic conductivities may violate the Forchheimer assumption in Darcy's equation, and require further analysis using turbulent flow equations. The dashed line represents the aquifer hydraulic conductivity used in the analysis.

With an effective well conductivity of 100 m/d, and a production zone with a transmissivity of 2.1 m²/d (21 m thick with conductivity of 0.1 m/d), the formation does have the capacity to transport water to the leaky well without limiting its flow. Flow would be limited when K_h is 0.01 m/d or less. Projecting this non-limiting case onto Figure 5 shows that the aquitard K_{eq} would significantly change from its background value if the following conditions are met: for a background aquitard K equal to 10⁻⁴ m/d when the number of leaky wells/km² is larger than or equal to one; for a background aquitard K equal to 10⁻⁵ m/d when the number of leaky wells/km² is larger than or equal to 0.1, etc.

For a fully open well, the aquifer will limit flow for an aquifer conductivity less than 100 m/d (Figure 7, the point at which the solid line levels off). This is a very high conductivity, typical for sands and gravel, but not representative for major aquifers such as the Pilliga Sandstone [CDM Smith 2014] in NSW. Therefore, for all instances where an open well is present in the system, flow is likely to be limited by aquifer conductivity. In other words, flow through an open well is governed by aquifer parameters, not by the parameters of the well. Because flow through a fully open well will be at least equal to or higher than flow through a leaky well ($K_{well} = 100$ m/d), the effect of such open wells on modifying the background conductivity of an aquitards will be at least as important as for the leaky well with $K_{well} = 100$ m/d. Therefore, fully open wells have the capacity to significantly change the hydraulic conductivity of an aquitard.

In the case of a well leaking through the degraded cement annulus ($K_{well} = 0.1$ m/d), flow is limited solely by the flow through the well for all realistic values of aquifer conductivity (Figure 7, dot-dash line). The conditions for which the background equivalent conductivity of an aquitard becomes significantly modified are shown in Figure 8: for a broad range of aquitard conductivities (10⁻² to 10⁻⁶ m/d), the number of leaky wells/km² has to be larger than five. Because this is highly unlikely, the

conclusion is that a leaky well with a degraded cement annulus ($K_{\text{well}} = 0.1 \text{ m/d}$) would not normally modify the equivalent hydraulic conductivity of an aquitard.

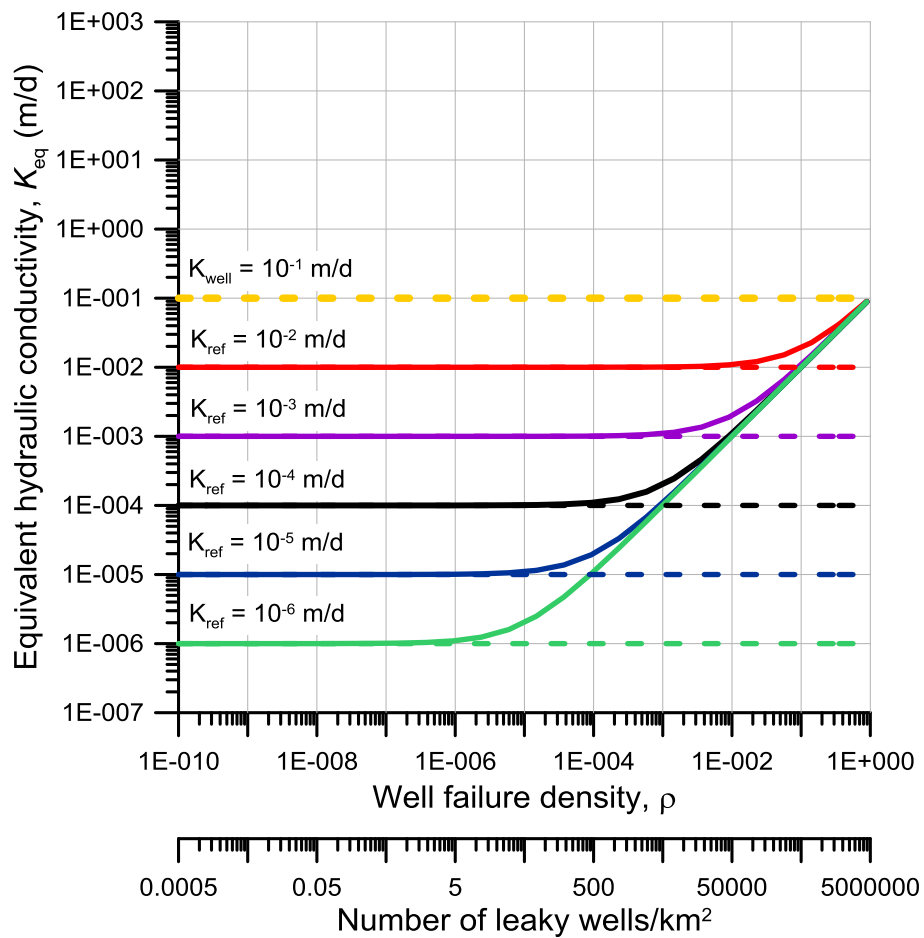


Figure 8 Equivalent hydraulic conductivity of an aquitard with a series of leaky wells ($K_{\text{well}} = 0.1 \text{ m/d}$) as a function of well failure density.

These analytical equations provide a broader parameter space and conceptualisations to assess the potential for flow through a leaky CSG well or water bore. However, they do not include the leakage and storage effects of the thick aquitard that separates the production zone and surface alluvial aquifer. Numerical modelling of the problem is warranted to assess these effects, therefore a numerical model with a more limited parameter space that is representative of real world conditions is subsequently applied to the problem.

3 Numerical model development

A single well groundwater flow model was developed to represent a three layer system, which is a simplification of the hydrogeological structure of the proposed Narrabri CSG development area, NSW. The model was developed in MODFLOW USG [Panday et al., 2013], using a Voronoi unstructured grid developed using AlgoMesh [Merrick, 2015].

The model domain consisted of an upper, confined water bearing aquifer, 114 m in thickness (Layer 1), a series of aquitards represented as a single layer of 600 m thickness (Layer 2) and an underlying, 21-m-thick aquifer comprising the coal seam targets used for CSG production (Layer 3) (Figure 9). The total thickness of the model was 735 m. To reduce the influence of boundary conditions, the model domain was defined as a 10,000 m radius around the gas production well. The Voronoi mesh was defined to have a maximum horizontal cell dimension of 750 m for the majority of the model and minimum horizontal cell dimensions at the production well. The minimum cell dimensions vary from 0.5 m to 1000 m to assess the impact of discretisation on flow in a leaky bore.

Horizontal and vertical hydraulic conductivity, specific yield and specific storage for each of the layers are shown in Table 2. For the basic model conceptualisation, initial conditions were defined by a 49 m downward head difference, being the largest pre-production head difference found in the Narrabri model [CDM Smith, 2014]. The head difference in both upward and downward gradients was varied for other scenarios as shown below. At a 10,000 m radius from the production bore, Layer 1 had a constant head boundary (CHB) of 328 m and Layer 3 had a CHB of 279 m, applied across the depth of the layer, while Layer 2 had a no-flow boundary condition at its perimeter.

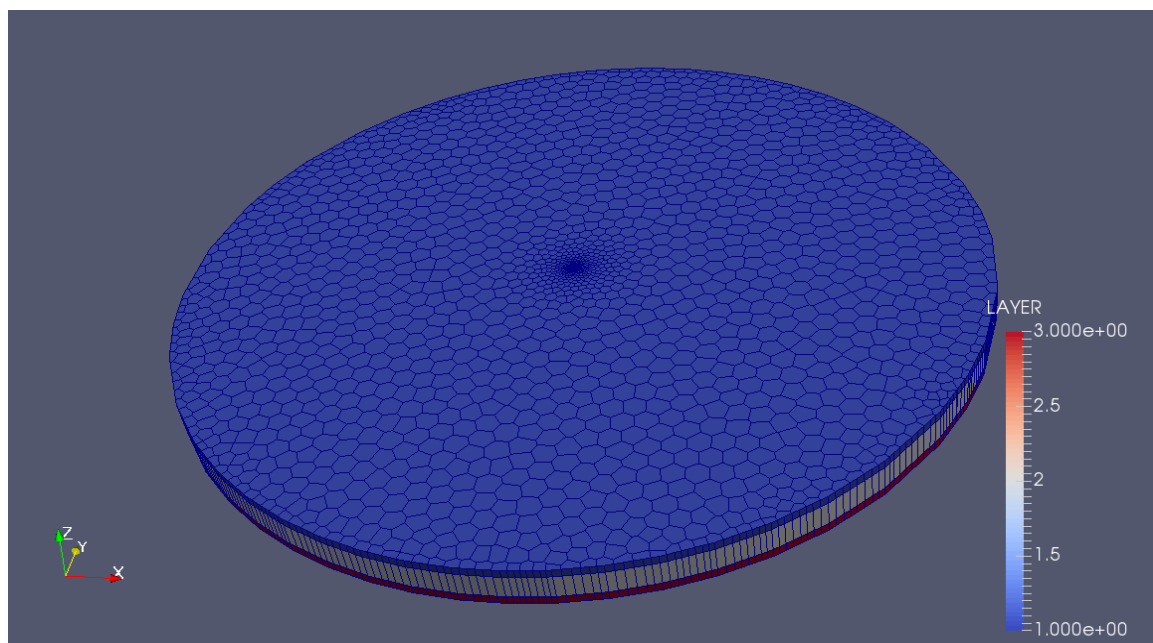


Figure 9 Model domain in AlgoMesh indicating the three model layers and grid refinement around the well at the centre of the domain.

The horizontal (K_h) and vertical (K_v) hydraulic conductivities for each of the model layers were sourced from the CDM Smith [2014] Narrabri models, with the median value used as bulk properties

in the aquitard (Layer 2) (Table 2). Specific yield (S_y) and specific storage (S_s) were also taken from the CDM Smith [2014] model, to be representative of actual hydrogeological properties. A well skin factor of 10 was used to reduce the sharp change in hydraulic conductivity between the well and the surrounding rock or soil matrix.

Table 2 Model parameters sourced from the CDM Smith [2014] Narrabri model. Parameters are defined in the text.

Parameter	Layer 1	Layer 2	Layer 3	Leaky well (scenario 2)	Open well (scenario 3)
Thickness (m)	114	600	21	-	-
Top elevation (mAHD)	363	249	-351	-	-
Base elevation (mAHD)	249	-351	-372	-	-
Constant head boundary (CHB) outer (m)	328	-	279	-	-
Horizontal hydraulic conductivity K_h (m/d)	0.1	0.001	0.1	-	-
Vertical hydraulic conductivity K_v (m/d)	0.01	1E-05	0.01	-	-
Specific yield S_y (-)	0.01	-	-	-	-
Storativity S_s (1/m)	1E-05	1E-05	1E-05	-	-
Length of leaky well (m)	-	-	-	735	735
Well radius r_w (m)	-	-	-	0.25	0.25
Effective well conductivity K_{well} (m/d)	-	-	-	8.13E-01	6.25E08
Constant head boundary for the initial production well CHB (m)	-	-	-	211	211
Well skin factor (-)	-	-	-	N/A	10

The system was first modelled in steady-state to find the pre-production quasi-equilibrium, then followed by transient simulations of the proposed 26 year gas production period. Final head distributions at the end of the gas production period were used as starting condition to simulate post-production hydraulic conditions that characterise the aquifer recovery period.

Groundwater heads during the production period were estimated by applying a 211 m CHB condition at the base of layer 3 at the production well for a period of 26 years; the head difference with aquifer 1 is $328-211=117\text{m}$. The simulated heads at 26 years were used as initial heads for modelling the groundwater recovery process.

The leaky well was conceptualised using the continuous linear network (CLN) package from MODFLOW-USG. The CLN package allows longitudinal flow through conduits that are much smaller than the model cell to be represented without the need for additional detail to be built into the mesh [Panday et al., 2013]. It also facilitates passive flow through a conduit, which is governed by the head gradient along the conduit and the resistance to flow through the conduit (K_{well}), between the conduit and the aquifer matrix (skin factor), and through the connected aquifers (K_{aq}).

Recovery of groundwater heads in the post-production period was modelled for three scenarios: (i) a perfectly sealed well at decommissioning which does not present a seepage pathway, (ii) a leaky well that is considered to be a major seepage pathway, and (iii) a well that represents a repurposed water bore (fully open well). Scenario 1 represents aquifer 2 recovery through replenishment from the aquitard (an intrinsically slow process) and from the model boundary conditions; recovery of aquifer 1 is only from the model boundary conditions. Note that recharge from diffuse rainfall was not considered in these scenarios. Scenario 2 represents flow through a leaky well with an effective well conductivity (K_{well}) of $8.13 \times 10^{-1} \text{ m/d}$, or 1100 mD, which was chosen to be conservatively one order of magnitude greater than that used by Nordbotten et al. [2009] (Table 2). The final scenario considers a fully open and leaky well which represents the greatest potential for inter-aquifer connectivity due to the very high conductivity assigned to the borehole (Table 2). An effective well conductivity of $6.25 \times 10^8 \text{ m/d}$ was used to represent the maximum limit of well conductivity, from an example well problem in Panday et al. [2013]. Flow through the well was found to be insensitive to effective conductivities at values greater than 4×10^4 . A skin factor of 10 was used to smooth the hydraulic conductivity difference between the groundwater cells and the well.

The groundwater model is set up to produce the following simulation metrics: (i) the relative contribution to inter-aquifer groundwater exchange from leaky, abandoned or repurposed CSG wells versus flow through aquitards, (ii) the sensitivity of aquifer recovery time in the post-production phase to various hydrogeological parameters, and (iii) the (maximum) head changes during or after the gas extraction phase. Scenario 1 will serve as the baseline condition against which the two other scenarios will be compared. In this way the effect of a leaky well (scenario 2) and an open borehole (scenario 3) on the simulation metrics will be quantified.

The first metric is concerned with the flux of water through a leaky, abandoned or repurposed CSG well between the water bearing aquifer and the production interval, compared with the flux of water through the aquitard. Three different head differences between layers 1 and 3 were modelled in steady-state using the parameters in Table 2. The head differences of 49 m downward and 25 m in an upward direction represented the largest head differences in each direction prior to CSG production [Wu et al., 2018]. The head difference of 115 m downward represented the maximum head difference immediately after CSG production ceased [Wu et al., 2018]. To test for sensitivity within the bounds of realistic parameters in the field, the model was also run using a lower aquitard hydraulic conductivity, and a higher aquifer conductivity. The one order of magnitude lower aquitard (Layer 2) K_h and K_v , represents a less permeable matrix between the aquifers, and a one order of magnitude higher aquifer (Layers 1 and 3) K_h and K_v represents a more permeable aquifer compared to the reference condition.

The second metric is about recovery of groundwater heads over time in the post-production phase. Groundwater recovery was modelled for a period of 1000 years, and the head drawdown around the well was extracted from the MODFLOW-USG simulations. Time series of groundwater head were developed at distances of 0 m, 10 m, 100 m and 1000 m from the production well. The aquifer

recovery time t_r was defined as the duration of time between ceasing production and the groundwater head reaching the pre-production head, if at all, at the point of interest.

The third metric is the maximum head changes at different distances from a well during the post-production phase. Groundwater recovery was modelled for 1000 years, and the drawdown curve away from the production well was plotted immediately after production ceased for times of 1 day, 1 year, 10 years, 100 years and 1000 years.

To determine what level of horizontal cell size would be acceptable when a few hundred CSG wells would be implemented in a regional groundwater model, the single-well model was run with minimum cell dimensions of 0.5 m, 1 m, 10 m, 50 m, and 1000 m around the leaky bore. The 1000 m minimum cell discretisation represents the cell dimension of a typical regional groundwater model, and the minimum cell dimensions was the same as the 0.5-m-diameter well.

A numerical model for the same system was also developed in MODHMS using the fracture well package (FWL4) [HydroGeoLogic, 2006] to evaluate the difference between the modelling code, and an appropriate discretisation around the wells. A three-layered model was constructed with the total length of the domain set to 10 km. Scenarios were constructed for minimum discretisations of 0.1, 1, 10, 100 and 1000 m. Based on an axi-symmetrical model, the spatial step was coarsened by 10% for each additional column until the final grid size had been reached. An axi-symmetric approach was used to simulate the pumping well. The same properties and head boundaries of the MODFLOW-USG model were adopted for the model MODHMS. The specified properties of the fracture well were implemented to be the same as the properties of the CLN used in the MODFLOW-USG model without a well skin value. Flow through the leaky well was compared between both MODHMS and MODFLOW-USG model, and for each minimum cell discretisation.

4 Results

4.1 Comparison numerical - analytical solutions

It is not possible to directly compare the results from the analytical equations and the numerical model, as the numerical model conceptualisation and parameters void some of the assumptions of the analytical equations. Most critically, the numerical model assumes that a semi-permeable aquitard separates the two aquifers, while the second series of analytical equations (9-18) assume a completely impermeable separation. The numerical model has an unconfined water bearing aquifer (Layer 1), while the analytical equations were written specifically for confined conditions.

It is possible though to obtain outputs from the numerical model that are similar to the analytical results using extremely low aquitard hydraulic conductivity values to simulate an impermeable aquitard, and a fully saturated layer 1. Alternatively, reducing the thickness of layer 1 in the analytical model to represent drawdown around the well will produce similar flow rates down the leaky or open well.

4.2 Impact of cell dimensions

For the parameter set described in Table 2, flow through the well was similar for all localised minimum cell dimensions using MODFLOW-USG with the CLN package representing the open well, scenario 3 (Table 3). Some initial modelling with higher well flows and larger aquifer transmissivities indicated that flow through the open well increased for the 1 m and 0.5 m discretisation due to the larger head gradient closer to the well.

Table 3 Effect of mesh size on flow through an abandoned well (scenario 3).

Minimum cell dimension (m)	Flow through well using MODFLOW-USG / CLN package (m ³ d ⁻¹)	Flow through well using MODHMS / FWL4 package (m ³ d ⁻¹)
0.5	22.6	34.6
1	22.5	37.2
10	22.6	49.1
100	22.5	72.1
1000	22.5	131.4

In contrast, flow through the well using MODHMS and the FWL4 package increased as the minimum cell dimension grew larger. This is because although the FWL4 package requires a well radius as an input, it does not use this radius to reduce the well flow due to converging flow lines within the groundwater cell associated with the well [Neville and Tonkin, 2001]. Neville and Tonkin [2001] suggest that for the results from the FWL4 package to match the results of the exact solution, the model grid must be refined as close as possible to the dimension of the actual well radius. It is unclear why they are not identical at a minimum cell dimension of 0.5 m.

If MODHMS and the fracture well (FWL4) package are used in the regional model, then localised grid refinement around each well, equal to the actual well radius, is required.

4.3 Metric 1: Comparison between flow through the well and flow through the aquitard

Comparison between flow through a leaky well, flow through an open well and regional leakage through the aquitard per square kilometre is shown in Table 4 to Table 6. The 1 kilometre square area for which aquitard leakage was calculated was based on a density of one CSG well per km² as described for the Narrabri Gas Project Area by CDM Smith [2014].

Table 4 Comparison between flow through a leaky and fully open well compared with regional flow through the aquitard, using parameters shown in Table 2 and a steady-state model.

Head difference between Layers 1 and 3 (m)	Flow through leaky well (m ³ /d)	Flow through open well (m ³ /d)	Regional leakage through aquitard (m ³ /d/km ²)	Ratio of leaky well flow to aquitard leakage	Ratio of open well flow to aquitard leakage
49 (downward)	7.6x10 ⁻³	22.5	0.60	1.26E-02	37.2
-25 (upward)	-4.2x10 ⁻³	-11.6	-0.34	1.24E-02	34.4
115 (downward)	1.7x10 ⁻²	51.4	1.41	1.21E-02	36.5

Table 5 Comparison between flow through a leaky and open well compared with regional flow through the aquitard, for one order of magnitude lower aquitard (Layer 2) K_h and K_v values and a steady state model. Flow through the leaky well is slightly higher in this example because the decreasing aquitard conductivity restricts flow through the aquitard in favour of flow through the well, just as turning off one tap will increase flow slightly through other taps in a multi-tap system.

Head difference between Layers 1 and 3 (m)	Flow through leaky well (m ³ /d)	Flow through open well (m ³ /d)	Regional leakage through aquitard (m ³ /d/km ²)	Ratio of leaky well flow to aquitard leakage	Ratio of open well flow to aquitard leakage
49 (downward)	8.8x10 ⁻³	24.3	0.07	1.34E-01	368.8
-25 (upward)	-4.9x10 ⁻³	-12.6	-0.04	1.33E-01	341.2
115 (downward)	2.1x10 ⁻²	55.9	0.15	1.36E-01	361.3

Table 6 Comparison between flow through a leaky and open well compared with regional flow through the aquitard, for one order of magnitude higher aquifer (Layers 1 and 3) K_h and K_v values and a steady-state model.

Head difference between Layers 1 and 3 (m)	Flow through leaky well (m ³ /d)	Flow through open well (m ³ /d)	Regional leakage through aquitard (m ³ /d/km ²)	Ratio of leaky well flow to aquitard leakage	Ratio of open well flow to aquitard leakage
49 (downward)	8.8x10 ⁻³	243	0.66	1.34E-02	368.8

-25 (upward)	-4.9×10^{-3}	-126.4	-0.37	1.33E-02	342.3
115 (downward)	2.1×10^{-2}	559	1.55	1.36E-02	361.3

Using the parameters in Table 2, flow through a leaky well was around 1% of the flow of water from the water bearing aquifer to the production zone through the aquitard (Table 4). The flow through a fully open well was around 35 times greater than the regional flow through the aquitard.

A decreased aquitard conductivity of one order of magnitude resulted in a one order of magnitude higher leakage ratio for scenario 2 and 3. Flow through the leaky and open wells was only slightly larger as it is dependent on the relative conductivity between the well and aquitard, but aquitard leakage was decreased. Increasing the aquifer conductivity by one order of magnitude also increased the leakage ratio for the open well, but not as much for the leaky well. For the leaky well (scenario 2) it appears that flow through the well is limited by the well conductivity rather than aquifer transmissivity. The open well (scenario 3) with the much higher effective well conductivity, is limited by the transmissivity of the aquifers, layers 1 and 3. This behaviour is similar to that described by the analytical equations in Figure 7.

From the analytical solution equation 15 and the parameters from Table 2, the effective hydraulic conductivity of the well required so that inter-aquifer flow is controlled by aquifer transmissivity, is $K_{\text{well}} = 4 \times 10^4$ (m/d). The effective well conductivity used for Scenario 3, the open well, is greater than this, while the effective well conductivity of a leaky bore is likely to be many orders of magnitude lower.

From equation 8, 621 leaky wells with K_{well} of 8.2×10^{-2} are required per square kilometre to significantly change the average vertical hydraulic conductivity of the regional system. As the flow through the open well is limited by the aquifer transmissivity, the effective hydraulic conductivity of the system is 4×10^4 m/d, based on the limit from Figure 7. At this effective conductivity, 1.2×10^{-3} bore per square km are required, which means that the presence of a single open well will impact the rate of water flow between alluvial and production aquifers.

4.4 Metric 2: Impacts of the leaky well on aquifer recovery

The heads in layer 1 were minimally affected by pumping during the 26 year production period. Any head variation was due to the loss of water through the well to layer 3, or diffuse leakage of water through the aquitard, layer 2. Nearly all of the head variation that was observed occurred during the post-production period.

Layer 3 was drawn down during the production period and had an observable recovery period after production ceased. After recovery, there is a very slow decline in head due to flow out of the constant head boundary at the furthest extent of the model. In reality this would not occur due to groundwater recharge at the model surface and inflows to the system from adjacent parts of the regional aquifer system. Groundwater recharge and interactions between different parts of the larger system will be explored in the regional groundwater modelling activity of this project.

4.4.1 Scenario 1: baseline without leaky wells

For the system with a perfectly sealed well, there was no discernible variation in heads in layer 1 after production ceased (Figure 10). Recovery of the layer 3 production aquifer in this example occurred after around two years (Figure 11). Drawdown of the aquifer was observed at distances of up to, and presumably over, 100 metres, but not as far as one kilometre. At one kilometre distance from the production well, the starting head is higher, due to the initial head input from the steady

state model run. The long term equilibrium head near the well in layer 3 was slightly higher than at the model boundaries due to the slow leakage of water from layer 1 through the aquitard. Over time, this head declines as the water replenishes the drawdown caused by production.

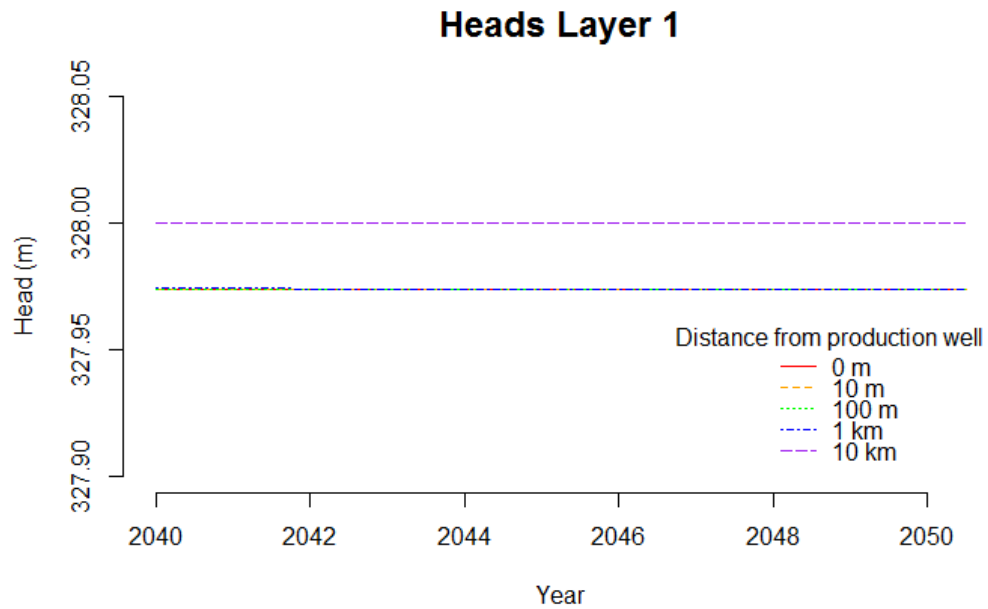


Figure 10 Time series of groundwater head in layer 1 at the production well and at 10 m, 100 m, 1 km, and 10 km from the production well, scenario 1 – perfectly sealed well. The year 2040 is the start of the post-production phase.

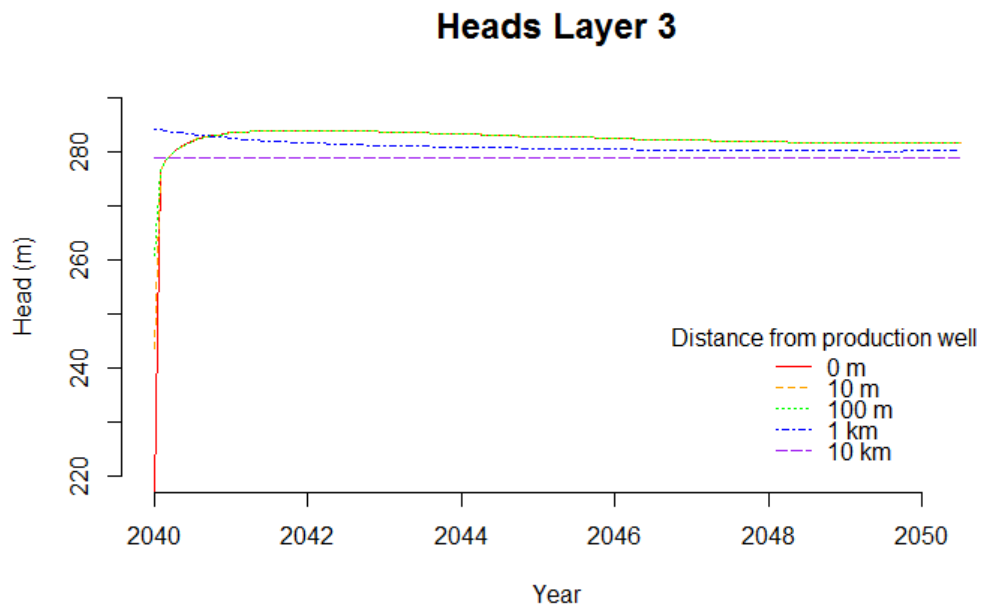


Figure 11 Time series of groundwater head in layer 3 at the production well and 10 m, 100 m, 1 km, and 10 km from the production well, scenario 1 – perfectly sealed well.

4.4.2 Scenario 2: Leaky well

The head time series for scenario 2, the leaky well (Figure 12, Figure 13), was almost identical to scenario 1 (Figure 10, Figure 11). Note the very small y-axis scale in Figure 12.

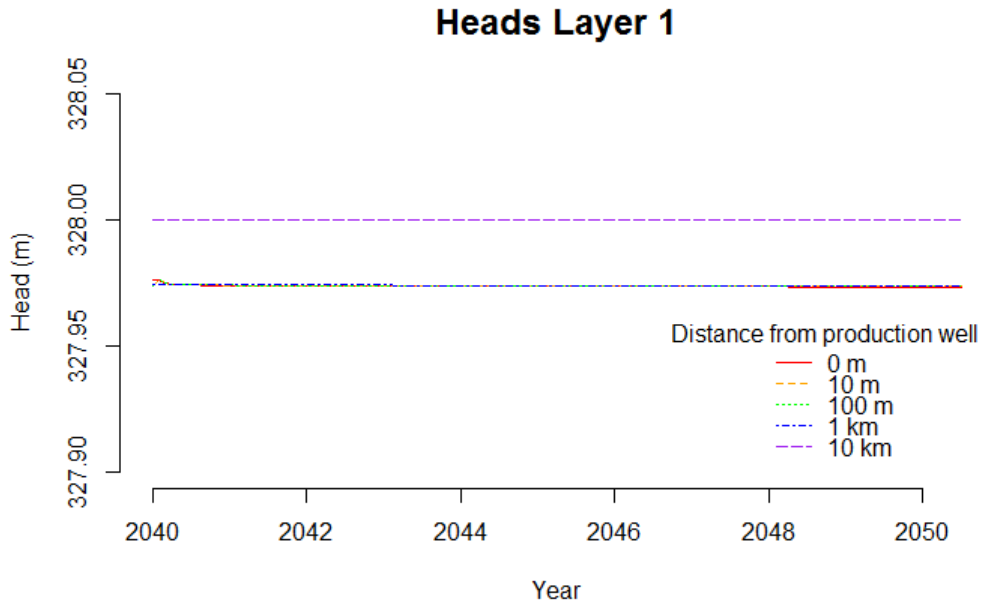


Figure 12 Time series of groundwater head in layer 1 at the production well and 10 m, 100 m, 1 km, and 10 km from the production well, scenario 2 – leaky well.

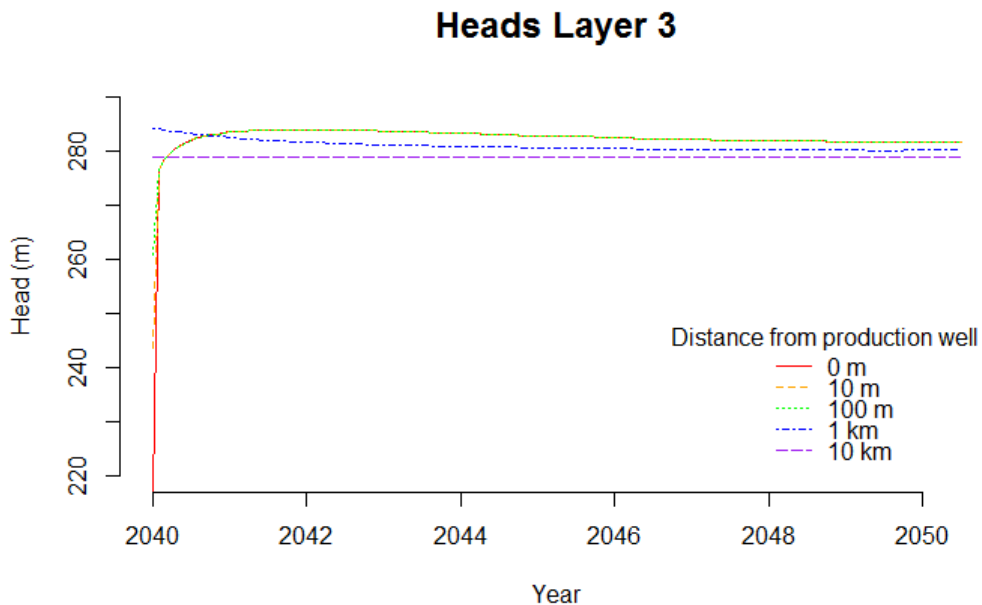


Figure 13 Time series of groundwater head in layer 3 at the production well and 10 m, 100 m, 1 km, and 10 km from the production well, scenario 2 – leaky well.

4.4.3 Scenario 3: Open well

For the open well scenario, there is a rapid decline in the groundwater heads of layer 1 at distances from the well of 100 m or less (Figure 14). The initial head decline is around five metres at the well, two metres at a distance of ten metres from the well, and around 1 metre 100 m from the well. After the initial decline, all locations up to 1 km from the open well slowly decline due to a slow leakage through the well and the regional aquitard. In 2050, 10 years post-production, all areas of the water bearing aquifer other than the constant head boundary have been drawn down to less than their pre-production levels, ranging from five metres close to the open well to around half a metre at one kilometre from the well. In a real situation, diffuse recharge is likely to compensate for the declines in the aquifer more distant from the open well. Recharge will be included in the regional groundwater model which is designed to investigate the cumulative impacts of a number of leaky wells in a CSG development.

As for the other scenarios, the groundwater head in layer 3 is again influenced by pumping in the production phase to a distance of over 100 m and less than 1 km (Figure 15). There is a rapid initial recovery of groundwater heads in layer 3 in the first few days after production pumping had ceased. After the initial recovery, the piezometric head continues to recover to levels above the initial pre-production heads for around two years. The new, higher heads are up to 22 m higher than pre-production levels at the open well, and around ten metres higher at a distance of 100 m from the well. Compared with the five metre head increase from scenario 1 (Figure 11) which was due solely to diffuse leakage through the aquifer, there is a maximum 15 m head increase which is attributable to the presence of the open well.

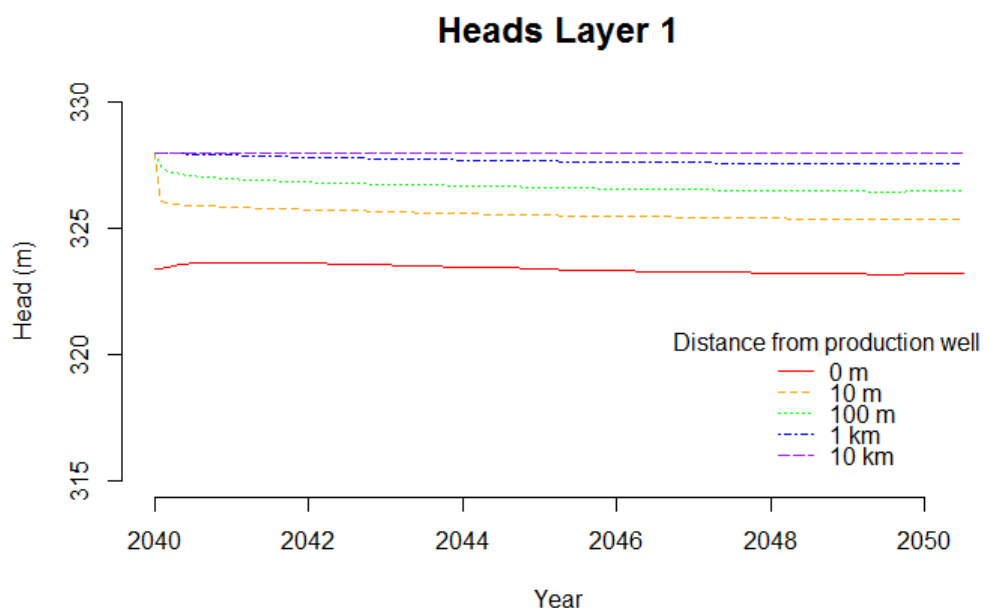


Figure 14 Time series of groundwater head in layer 1 at the production well and at 10 m, 100 m, 1 km, and 10 km from the production well, scenario 3 – open well.

Heads Layer 3

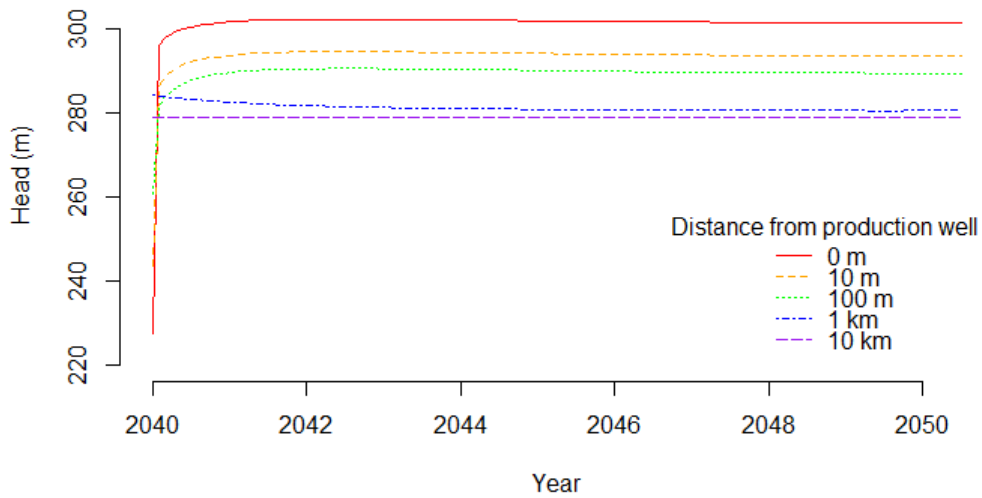


Figure 15 Time series of groundwater head in layer 3 at the production well and 10 m, 100 m, 1 km, and 10 km from the production well, scenario 3 – open well.

4.5 Metric 3: head changes around a well

There is minimal evidence for drawdown associated with a flow down a failed CSG well for scenarios 1 and 2, i.e. fully sealed and leaky wells. In these cases, flow through the well is insignificant compared with regional leakage through the aquitard. In comparison, there is a concerning drawdown in the water bearing aquifer due to the presence of a fully-open exploration or repurposed bore.

4.5.1 Scenario 1: baseline without leaky wells

Groundwater head drawdown around the production well for scenario 1, the fully sealed well, show no cone of depression in layers 1 or 2 (Figure 16 and Figure 17). There is a small regional drawdown in layer 1 (<0.1 m) and moderate drawdown (1 m) in layer 2 after 1000 years. In contrast, heads in layer 3 are around 20 m *higher* than pre-production levels after 1000 years.

Heads L1

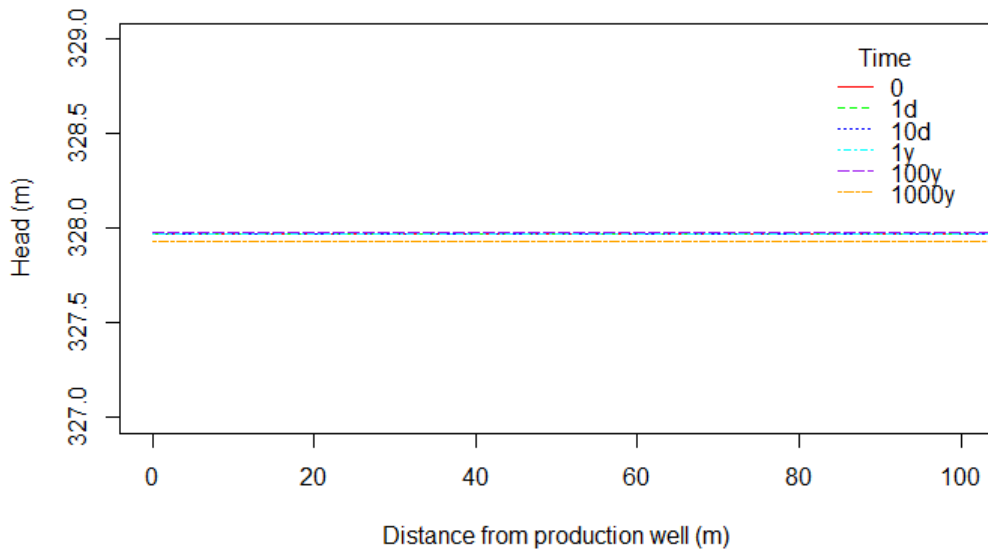


Figure 16 Groundwater head drawdown cones in layer 1 with delays of between 0 and 1000 years post-production, for the fully sealed well, scenario 1.

Heads L2

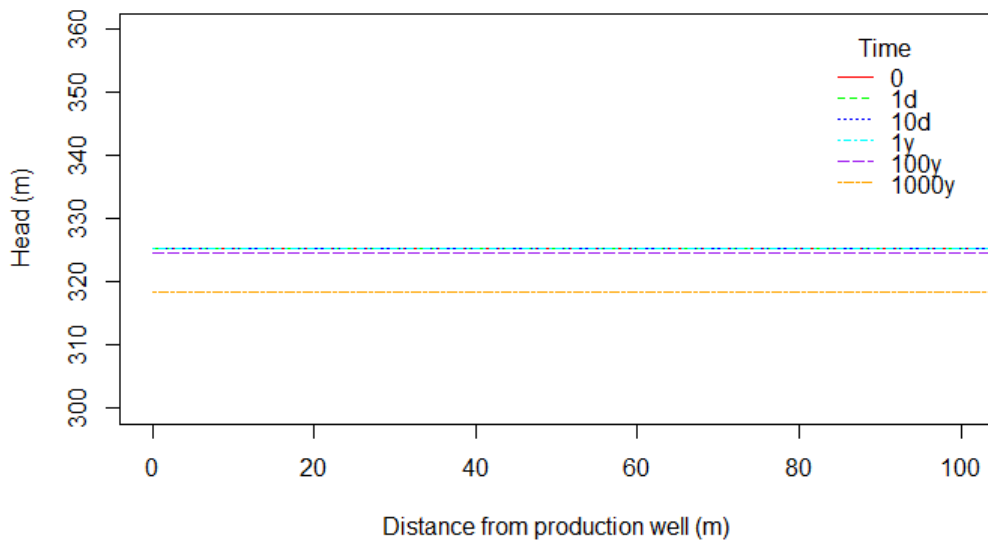


Figure 17 Groundwater head drawdown cones in layer 2 (aquitard) with delays of between 0 and 1000 years post-production, for the fully sealed well, scenario 1.

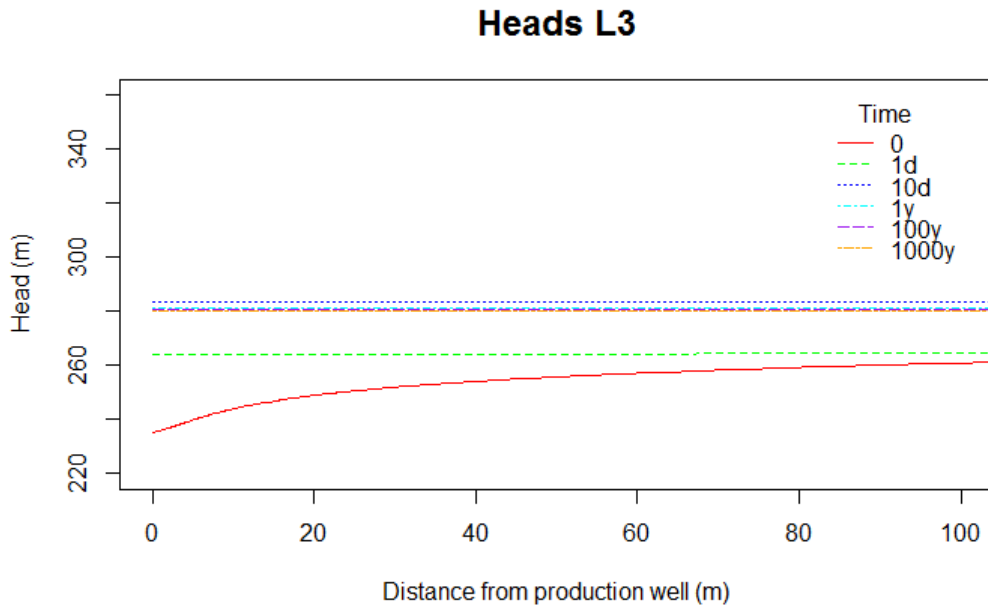


Figure 18 Groundwater head drawdown cones in layer 3 (aquifer) with delays of between 0 and 1000 years post-production, for the fully sealed well, scenario 1

4.5.2 Scenario 2: Leaky well

Drawdown in layer 1 for the leaky well, scenario 2, was minimal, i.e. less than 0.3 m over 1000 years (Figure 19). The overall decline can be attributed to both discrete leakage through the compromised production well and diffuse leakage through the aquitard.

Heads in the aquitard, layer 2, display a 0.3 m localised drawdown within 10 metres of the well that can be attributed to leakage through a compromised well casing or annulus (Figure 20). However, this is insignificant compared with the drawdown of 17 m, 1000 years after production ceased due to diffuse water loss from the aquitard to replenish the production interval, layer 3. Within a realistic timeframe of 100 years post production, the head decline of around one metre due to diffuse leakage is still greater than the drawdown due to the presence of the leaky well.

Head recovery in the production interval is similar to the completely sealed well, scenario 1 (Figure 21).

Heads L1

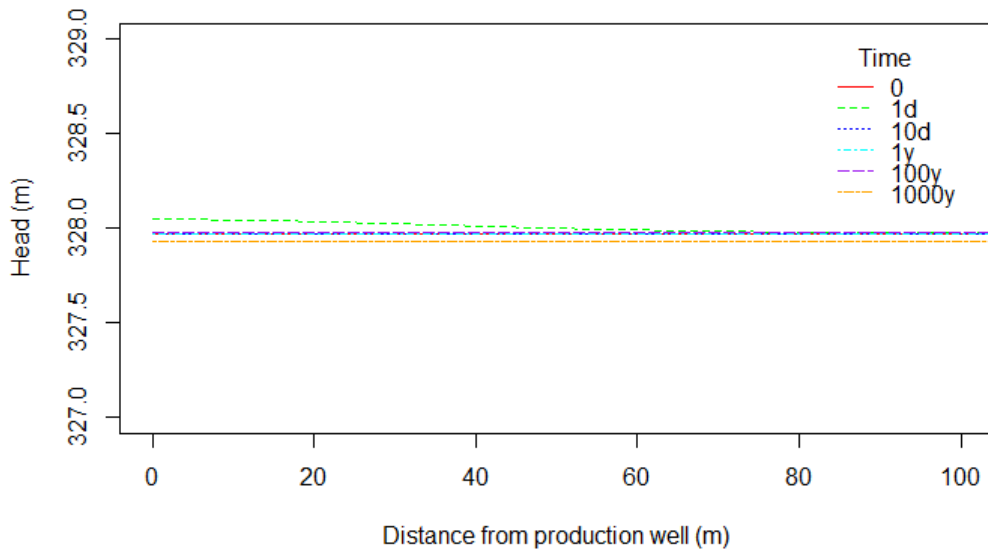


Figure 19 Groundwater head drawdown cones in layer 1 with delays of between 0 and 1000 years post-production, for the leaky well, scenario 2.

Heads L2

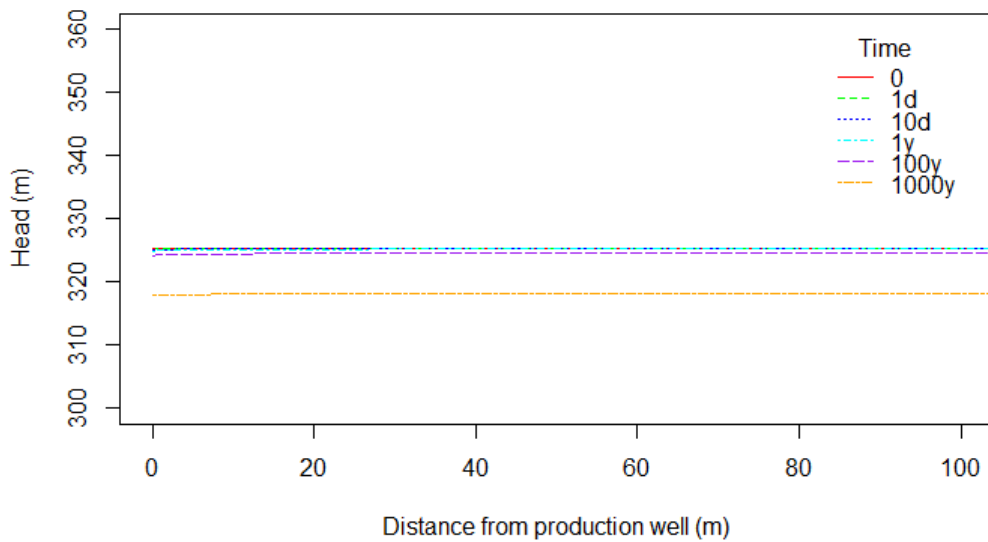


Figure 20 Groundwater head drawdown cones in layer 2 with delays of between 0 and 1000 years post-production, for the leaky well, scenario 2.

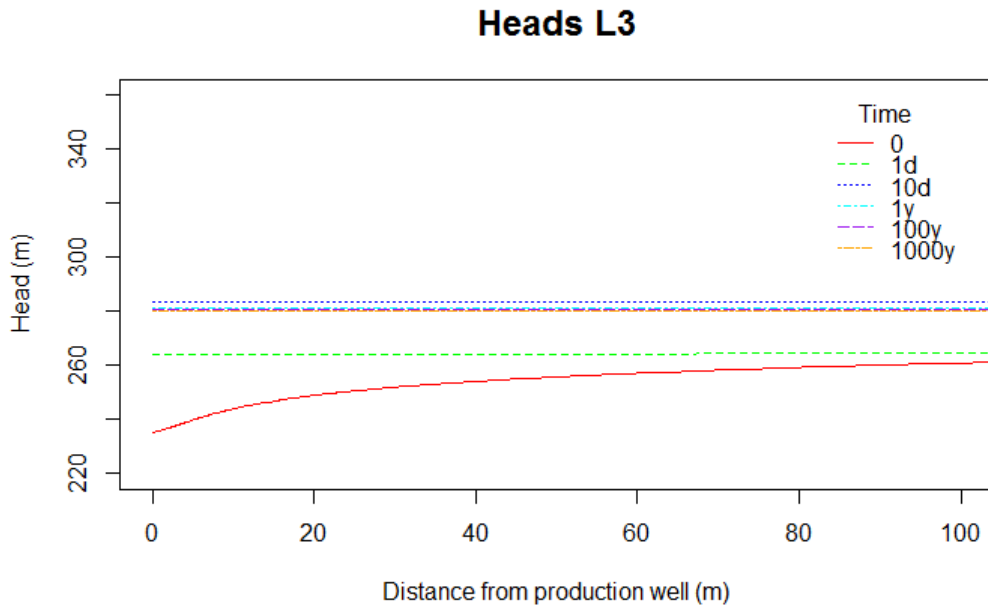


Figure 21 Groundwater head drawdown cones in layer 3 with delays of between 0 and 1000 years post-production, for the leaky well, scenario 2.

4.5.3 Scenario 3: Open well

Head drawdown in layer 1 for the open well, scenario 3, was up to five metres (Figure 22). Even for distances of more than 100 m from the production well, the likely decrease in piezometric level after 100 years was around 3.5 m. There is a rapid recovery close to the well within days of the cessation of production pumping, which propagates out beyond 100 m from the well within a year. Although this conceptualisation does not take into account regional groundwater recharge, it is likely that there will still be an impact on water levels within the vicinity of an open bore.

Recovery within the aquitard, layer 2, is also more rapid and extensive than the other scenarios (Figure 23), although the ultimate level at 1000 years post-production is similar.

An inverted cone of depression is present in the production interval due to water gains through the open bore (Figure 24). The initial head curve at $t=0$, which reflects the first modelled time step (1×10^{-3} days) demonstrates the rapid recovery of the production-induced drawdown, with a groundwater mound adjacent the bore which overlies the initial cone of depression.

Heads L1

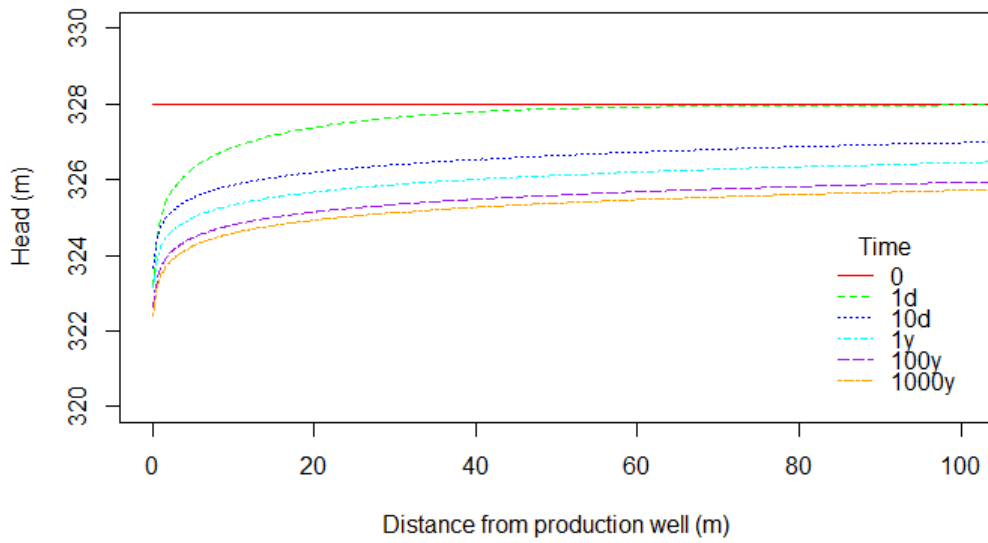


Figure 22 Groundwater head drawdown cones in layer 1 with delays of between 0 and 1000 years post-production, for the open well, scenario 3.

Heads L2

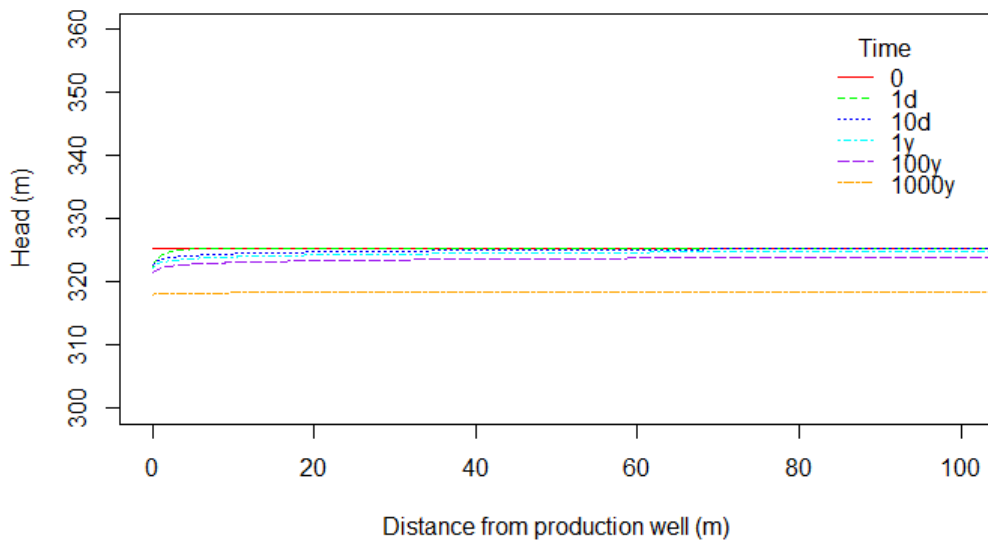


Figure 23 Groundwater head drawdown cones in layer 2 with delays of between 0 and 1000 years post-production, for the open well, scenario 3.

Heads L3

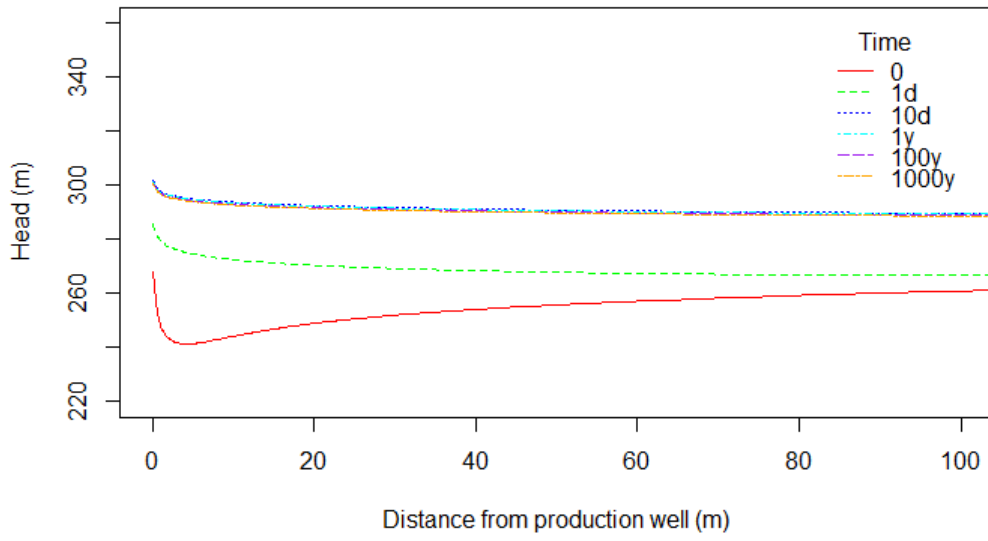


Figure 24 Groundwater head drawdown cones in layer 3 with delays of between 0 and 1000 years post-production, for the open well, scenario 3.

5 Discussion

While the hydrogeology of coal seam gas systems is usually conceptualised using dual- or multi-phase flow processes, there are instances where modelling the system using single-phase groundwater flow models is warranted for parsimonious reasons or due to budget constraints. It has been demonstrated that conceptualisation of groundwater flow problems associated with CSG production using single-phase models will over predict drawdown, as higher pressures are required to remove water from rock matrix where gas replacement is not modelled [Moore et al., 2014]. For this reason, the drawdown results from the single-phase groundwater flow modelling presented in this report will be conservative. If no impact is detected using the single-phase models presented, it is unlikely that the system will be impacted in reality. Similarly, if an impact is predicted, in reality the impact will be somewhat less than presented in this report, and multi-phase flow modelling may be necessary if exact quantification is required.

Both the generalised analytical solutions and the numerical modelling with a more specific parameter set described a three layer system with a leaky well, including water-bearing aquifer (layer 1), aquitard (layer 2) and a gas production zone (layer 3). Both analyses indicated that flow through the well is limited by either the effective conductivity of the well, K_{well} , or the transmissivity of the aquifers. For the site characteristics specific to one location within the projected production zone of the Narrabri model [CDM Smith, 2014] the effective well conductivity at which flow was limited by the aquifer capacity to transmit flow was around 4×10^4 m/d.

The numerical models used in the analysis, MODFLOW-USG with the CLN package and MODHMS with the FWL4 package, are similar in the way that they conceptualise the leaky well problem. Both models use a Darcy-type gradient equation to describe a well with radius less than the groundwater cell dimension in which they are located. Flow between the groundwater matrix and the well is also governed by the head difference and the presence of a resistive skin factor between the two. The results from the numerical models were of the same order of magnitude as flow calculated using the analytical equations, although the analytical equations did not include leakage through an aquitard, nor an unconfined surficial aquifer.

For the parameter set derived for the Narrabri region, the MODFLOW-USG / CLN model was not affected by the minimum cell discretisation, while flow through the well calculated by the MODHMS / FWL4 model increased with increasing cell size. Flow through a well calculated using MODHMS / FWL4 is only accurate when the local grid refinement around the well matches that of the actual well dimensions. If MODHMS and the fracture well (FWL4) package are used to develop the regional model, then localised grid refinement around each well, equal to the actual well radius, is required.

Flow through a leaky well in scenario 2 was around 1% of regional leakage through the aquitard for an area of one square kilometre, a relatively insignificant proportion. In comparison, flow through a fully open well was 35 times (3500%) that of aquitard leakage, which is likely to have a major impact on drawdown in the surficial aquifer. For a more resistive aquitard, the ratio of well to aquitard leakage increased to around 13%, predominantly due to the lowered aquitard leakage rather than the slightly increased flow through the well. If the aquifers were found to have a one order of magnitude higher hydraulic conductivity, only flow through the open well would increase, as aquifer transmissivity was the limiting factor for water movement in this case. This is in agreement with the analytical solutions in section 2.2.

Table 7 Summary of metrics for the three well scenarios

Scenario	Ratio of well flow to aquitard leakage (%)	Layer 1 drawdown at 50 yrs (m)	Layer 3 drawdown at 50 yrs (m)	Layer 3 recovery time (days)
Fully sealed (1)	0	0	0	730
Leaky (2)	1.2%	0	0	730
Open (3)	3500%	5	-15	5

The heads in the surficial aquifer and aquitard were not obviously affected by pumping during the 26 year production period. The production zone was drawn down due to pumping and had an obvious recovery period once production ceased. For the specific parameter set in Table 2, the full aquifer recovery time around the pumping - induced cone of depression was around 2 years for the two sealed and leaky well scenarios, and around 5 days for the open well. The open well scenario took around 2.5 years to stabilise to the new level, 15 m higher than before.

The presence of an open well caused drawdown of the surficial aquifer of between one metre and five metres from initial conditions within a distance of 100 m from the well. This drawdown was observed to be sustained for at least 50 years after production ceased, although in a real situation regional groundwater recharge may lead to a partial recovery of heads in the long term. The long term piezometric head in the gas production zone was higher than initial conditions due to the inflow of water from the open well.

For the fully sealed well and leaky well scenarios, the production-induced drawdown in layer 3 was in the main part relieved by the loss in storage and movement of water (and subsequent lowering in piezometric head) from the aquitard. In the open well scenario, the contributor to aquifer recovery was flow through the well, which resulted in a very rapid recovery in the vicinity of the well, followed by slower propagation of this water through the aquifer. A groundwater mound of approximately one metre was formed around the well.

The results of this modelling are specific to parameters describing one location of the Narrabri model, and do not include external processes such as groundwater recharge and flow between adjacent parts of the aquifers. The impacts of groundwater recharge and interactions between different parts of the larger system will be explored in the regional groundwater modelling activity of this project.

From the modelling described in this report, it is unlikely that there will be an impact from leaky, decommissioned CSG wells on a hydrogeological system similar to that of the Narrabri CSG region of the Gunnedah Basin. It is likely that exploration or repurposed production bores that remain open after the site is decommissioned will impact water levels in the surficial aquifer.

This analysis has been concerned with the movement of water between the aquifers and aquitards in a CSG production area. It does not include the movement of methane gas or solute transport associated with the flow of water. For areas with a natural upward hydraulic gradient, flow of water from the production zone to the water bearing aquifer is possible. This has the potential for contamination of the water bearing aquifer from lower-quality water in the production zone from higher TDS concentration or the remnants of fracking fluids and drilling mud.

6 Conclusions

Flow through an open or leaky well was found to predominantly be controlled by the effective well conductivity (ability to move water between aquifers via a connecting well) or the transmissivity of the aquifers (the ability of the aquifers to dissipate or provide water).

A high level of localised discretisation around each well is required in the regional, cumulative effects model if MODHMS and the fracture well (FWL4) package are used. Localised discretisation in this model needs to be the same as the well radius for the FWL4 package to avoid numerical error.

Flow through a single leaky well was insignificant when compared with vertical flow through a regional aquitard, but the flow through a fully open well was around 35 times greater than the regional vertical flow through the aquitard for the specific parameter set used in this study.

An effective well conductivity of at least 4×10^4 m/d was required before the system was controlled by the aquifer transmissivity. The presence of a single, fully open well will impact the rate of water flow between alluvial and production aquifers, whereas over 600 leaky bores per square kilometre are required to have a significant impact.

It is unlikely that there will be an impact from leaky CSG bores on the regional-scale hydrogeology of a system similar to that of the Narrabri CSG region of the Gunnedah Basin. However, it is likely that exploration or repurposed production bores that remain open after the site is decommissioned will impact water levels in the surficial aquifer. Further work is required to assess other potential impacts, such as aquifer contamination from methane transport or solute transport from the production zone in areas where an upward hydraulic gradients exist.

7 References

- Carey, J. W., M. Wigand, S. J. Chipera, G. WoldeGabriel, R. Pawar, P. C. Lichtner, S. C. Wehner, M. A. Raines, and G. D. Guthrie (2007), Analysis and performance of oil well cement with 30 years of CO₂ exposure from the SACROC Unit, West Texas, USA, *International Journal of Greenhouse Gas Control*, 1(1), 75-85.
- CDM Smith (2014), Santos Narrabri Gas Project: Groundwater modelling report. *Rep.*, 291 pp, Subiaco, WA.
- Connell, L., D. Down, M. Lu, D. Hay and D. Heryanto (2014), An assessment of the integrity of wellbore cement in CO₂ storage wells. Report prepared for Australian National Low Emissions Coal Research Development.
- Crow, W., J. W. Carey, S. Gasda, D. Brian Williams, and M. Celia (2010), Wellbore integrity analysis of a natural CO₂ producer, *International Journal of Greenhouse Gas Control*, 4(2), 186-197.
- Duguid, A., R. Butsch, J. W. Carey, M. Celia, N. Chuginov, S. Gasda, T. Ramakrishnan, V. Stamp, and J. Wang (2013), Pre-injection baseline data collection to establish existing wellbore leakage properties, *Energy Procedia*, 37, 5661-5672.
- Dusseault, M., and R. Jackson (2014), Seepage pathway assessment for natural gas to shallow groundwater during well stimulation, in production, and after abandonment, *Environmental Geosciences*, 21(3), 107-126.
- Flemisch, B., et al. (2011), DuMux: DUNE for multi-{phase, component, scale, physics, ...} flow and transport in porous media, *Advances in Water Resources*, 34(9), 1102-1112.
- Harbaugh, A. W. (2005), *MODFLOW-2005, the US Geological Survey modular ground-water model: The ground-water flow process*, US Department of the Interior, US Geological Survey Reston, VA, USA.
- Hawkes, C. D., and C. Gardner (2013), Pressure transient testing for assessment of wellbore integrity in the IEAGHG Weyburn–Midale CO₂ Monitoring and Storage Project, *International Journal of Greenhouse Gas Control*, 16, S50-S61.
- HydroGeoLogic (2006), MODHMS: A comprehensive MODFLOW-based hydrologic modeling system, Version 3.0. *Rep.*, HydroGeoLogic Incorporated, Herndon, VA.
- Jackson, R. B. (2014), The integrity of oil and gas wells, *Proceedings of the National Academy of Sciences*, 111(30), 10902-10903.
- Kissinger, A., R. Helmig, A. Ebigbo, H. Class, T. Lange, M. Sauter, M. Heitfeld, J. Klünker, and W. Jahnke (2013), Hydraulic fracturing in unconventional gas reservoirs: risks in the geological system, part 2, *Environmental earth sciences*, 70(8), 3855-3873.
- Lewicki, J. L., J. Birkholzer, and C.-F. Tsang (2007), Natural and industrial analogues for leakage of CO₂ from storage reservoirs: identification of features, events, and processes and lessons learned, *Environmental Geology*, 52(3), 457-467.
- Merrick, D. (2015), AlgoMesh: A new software tool for building unstructured grid models, in *Modflow and More 2015: Modeling a Complex World*, edited, Colorado School of Mines, Golden, Colorado, USA. May 31–June 3 2015.
- Moore, C. R., J. Doherty, S. Howell, and L. Erriah (2014), Some Challenges Posed by Coal Bed Methane Regional Assessment Modeling, *Groundwater*, 53(5).

Moridis, G. J., and C. M. Freeman (2014), The RealGas and RealGasH2O options of the TOUGH+ code for the simulation of coupled fluid and heat flow in tight/shale gas systems, *Computers & Geosciences*, 65, 56-71.

Neville, C. J., and M. J. Tonkin (2001), Representation of multiaquifer wells in MODFLOW, paper presented at Proceedings of Modflow 2001 Conference at the International Ground Water Modeling Center, Golden, Colorado.

Nordbotten, J. M., D. Kavetski, M. A. Celia, and S. Bachu (2009), Model for CO₂ leakage including multiple geological layers and multiple leaky wells, *Environmental science & technology*, 43(3), 743-749.

Nowamooz, A., J. M. Lemieux, J. Molson, and R. Therrien (2015), Numerical investigation of methane and formation fluid leakage along the casing of a decommissioned shale gas well, *Water Resources Research*, 51(6).

Panday, S., C. D. Langevin, R. G. Niswonger, M. Ibaraki, and J. D. Hughes (2013), MODFLOW–USG version 1: An unstructured grid version of MODFLOW for simulating groundwater flow and tightly coupled processes using a control volume finite-difference formulation, *Report Rep. 6-A45*, 78 pp, Reston, VA.

Reagan, M. T., G. J. Moridis, N. D. Keen, and J. N. Johnson (2015), Numerical simulation of the environmental impact of hydraulic fracturing of tight/shale gas reservoirs on near-surface groundwater: Background, base cases, shallow reservoirs, short-term gas, and water transport, *Water Resources Research*, 51(4), 2543-2573.

Schlumberger (2011), Manual for ECLIPSE Reservoir Simulation Software. *Rep.*, Houston, Texas.

Silliman, S., and D. Higgins (1990), An Analytical Solution for Steady-State Flow Between Aquifers Through an Open Well, *Groundwater*, 28(2), 184-190.

US EPA (2015), Assessment of the Potential Impacts of Hydraulic Fracturing for Oil and Gas on Drinking Water Resources. EPA/600/R-15/047a.*Rep.*

Vengosh, A., R. B. Jackson, N. Warner, T. H. Darrah, and A. Kondash (2014), A critical review of the risks to water resources from unconventional shale gas development and hydraulic fracturing in the United States, *Environmental science & technology*, 48(15), 8334-8348.

Wu, B., R. Doble, C. Turnadge, and D. Mallants (2018), Bore and well induced inter-aquifer connectivity: a review of literature on failure mechanisms and conceptualisation of hydrocarbon reservoir-aquifer failure pathways. Prepared by the Commonwealth Scientific and Industrial Research Organisation CSIRO, Canberra.*Rep.*